Orthopedic Research and Reviews

Dovepress
Taylor & Francis Group

Open Access Full Text Article

REVIEW

Enhancing Bone Repair with β-TCP-Based Composite Scaffolds: A Review of Design Strategies and Biological Mechanisms

Xuewen Ni[1–3,*], Jing Feng[2–4,*], Mengxue Liang[1–3], Fangzheng Zhou[1–3], Yuanjie Xia[1–3], Zijie Dong[1–3], Qingyu Xue[1–3], Zehao Li[1–3], Feifei Pu[2–4], Ping Xia[3,5]

[1]First Clinical College, Hubei University of Chinese Medicine, Wuhan, 430065, People's Republic of China; [2]Department of Orthopedics, Wuhan No.1 Hospital, Wuhan, 430022, People's Republic of China; [3]Department of Orthopedics, Traditional Chinese and Western Medicine Hospital, Hubei University of Chinese Medicine, Wuhan, 430022, People's Republic of China; [4]Department of Orthopedics, Traditional Chinese and Western Medicine Hospital of Wuhan, Tongji Medical College, Huazhong University of Science and Technology, Wuhan, 430022, People's Republic of China; [5]Department of Orthopedics, Wuhan Fourth Hospital, Wuhan, 430033, People's Republic of China

*These authors contributed equally to this work

Correspondence: Feifei Pu; Ping Xia, Email pufeifei@hust.edu.cn; xiapingfm@163.com

Abstract: It is reported that there are approximately 2.2 million bone graft procedures every year due to injuries, bone tumors, marginal bone defects, and aging of the population. However, the scarcity of natural donors and graft rejection make it difficult to adequately fulfill clinical demands for bone repair. While β-tricalcium phosphate (β-TCP) is a key material in bone tissue engineering, it remains insufficient for treating large bone defects. Therefore, researchers have started investigating the combination of β-TCP with other biomaterials to achieve improved clinical outcomes. Such composite scaffolds possess excellent biocompatibility and effectively provide structural support to promote cell adhesion, proliferation, and differentiation—thereby accelerating new bone tissue formation. This review examines β-tcp-based composite scaffolds for bone regeneration, analyzing design innovations and biological mechanisms, and bone repair principles—with a focus on cellular dynamics and microenvironmental regulation. The discussion valuates β-TCP's osteoconductive properties while addressing its clinical limitations in mechanical strength and degradation control. Additionally, it systematically elucidates the specific application of β-TCP-based composite scaffolds in bone repair. These include osteoinductive, osteogenic, osteoconductive and inflammatory regulation. Moreover, clinical translation progress is discussed, highlighting applications in craniomaxillofacial reconstruction and osteonecrosis management. Finally, we summarize that β-TCP composite scaffolds face challenges including poor mechanical strength, asynchronous degradation-regeneration, and manufacturing limitations. Future directions should focus on developing synchronously degradable materials and intelligent scaffolds via 4D printing and AI-optimized designs, and clinical translation systems to achieve precise bone regeneration.

Keywords: bone regeneration, bone defect, biomaterials, composite scaffold, β-tricalcium phosphate

Introduction

Between 2015 and 2050, the proportion of the world's population over 60 years will nearly double from 12% to 22%.[1] The accelerated aging of the global population has led to a notable increase in the incidence of bone-related diseases, often accompanied by serious complications.[2–5] Factors such as accidental trauma, bone tumors, and critical bone defects significantly contribute to the approximately 2.2 million bone grafts performed annually.[6,7] This not only severely affects the quality of life for patients but also imposes a substantial economic burden on society. In most cases, minor bone injuries (eg, cracks and certain types of fractures) can be repaired naturally without surgical intervention. However, spontaneous healing is rarely achieved in larger bone defects (2.5 cm or greater). Such defects may necessitate bone grafting techniques to facilitate recovery.[8–10] Autologous bone grafts are considered the "gold standard" for bone grafting due to their superior osteogenic properties, remarkable histocompatibility, and stable structural support.[11,12] However,

Received: 3 March 2025
Accepted: 7 June 2025
Published: 14 July 2025

this clinical application is limited due to the scarcity of donors and potential post-operative complications, such as pain, infection, fractures, and nerve damage. Allograft bone grafting is the second most common modality, but it also faces notable challenges, including limited donor resources, high costs, required sterilization and activation procedures, and the potential risk of viral disease transmission[13,14] Consequently, innovative solutions are urgently required to address the therapeutic needs of patients with bone defects. Identifying an ideal bone-grafting material is crucial for treating bone defects. Bone tissue engineering employs advanced principles and techniques to tackle this challenge.[15]

The degradation, resorption, and regeneration of implanted materials, along with the formation of new bone tissue, restore bone structure and function when implanted at the defect site.[21] Tissue-engineered bone has emerged as an ideal bone repair material due to its diverse range of material sources, high reproducibility, non-immunogenicity, and personalization. Primary sources include organic, inorganic, and composite bone materials (Figure 1).[22]

Composite materials are increasingly recognized as key biomaterials due to their superior performance, such as excellent biocompatibility,[23] tunable mechanical properties,[24] controllable degradability,[25] and enhanced osteogenic potential.[26] Among these, β-tricalcium phosphate (β-TCP) is highly favored for its resemblance to human bone.[27] Figure 2 illustrates the results of a Web of Science and PubMed database search for literature including "β-TCP" and "Bone defect" over the past decade. These results indicate the annual publication volume on β-TCP has remained relatively stable, and this biomaterial continues to demonstrate notable academic exploration value in the field of bone defect repair.

This review is based on the basic principles of bone repair and examines the biological properties of β-TCP, highlighting its advantages and limitations. Additionally, it introduces applications of β-TCP in various composite scaffolds, focusing on their enhancement of osteoinductivity, osteoconductivity, and osteogenesis, as well as their modulation of inflammatory responses and clinical uses. This review aims to summarize existing research achievements, provide valuable references and innovative ideas for further research and clinical applications of β-TCP materials, and systematically present its conceptual framework (Figure 3), which integrates key dimensions of β-TCP-based bone regeneration.

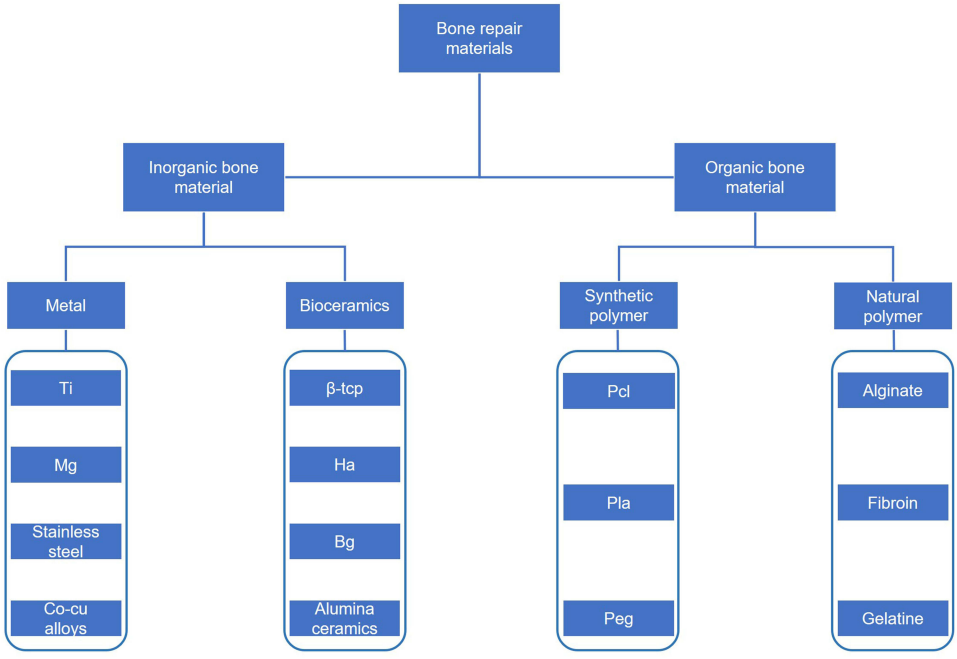

Figure 1 The main materials used in bone tissue engineering.

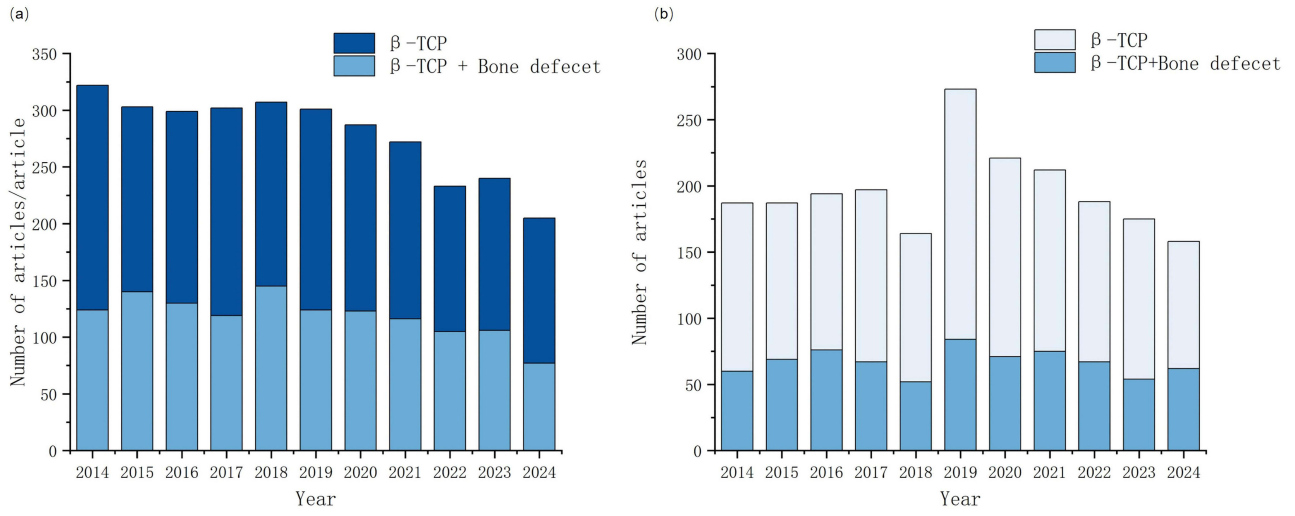

Figure 2 Results from PubMed (**a**) Results obtained from Web of Science (**b**).

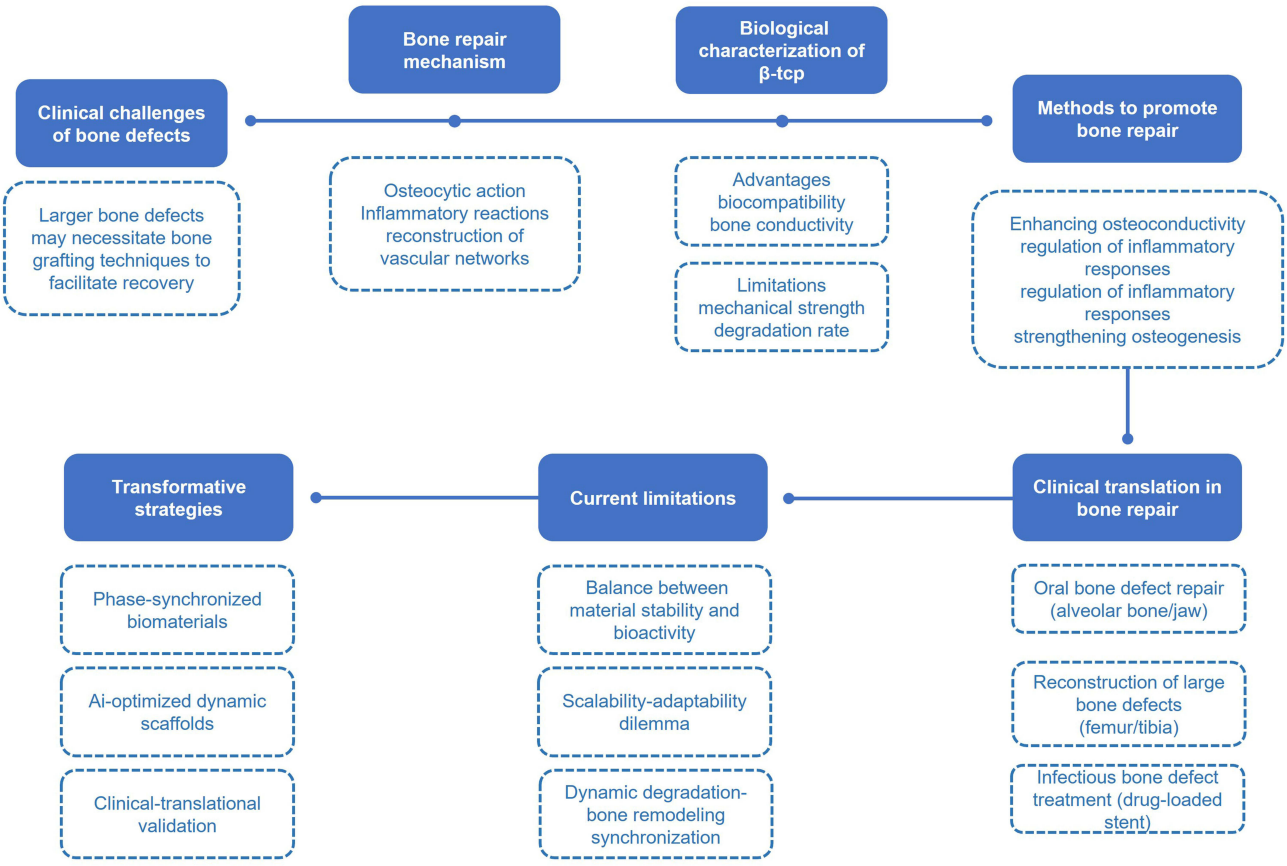

Figure 3 Engineering β-Tricalcium Phosphate Composite Scaffolds: Bridging Material Innovation, Biological Mechanisms, and Clinical Bone Regeneration.

Overview of Bone Repair

BMSCs Osteogenesis and Bone Cell Coupling in Regeneration

Osteoblasts and osteoclasts are the primary functional cells involved in bone formation and repair (Figure 4) and Osteoblasts are primarily differentiated from bone marrow mesenchymal stem cells (BMSCs) through BMP/TGF-β

https://doi.org/10.2147/ORR.S525959

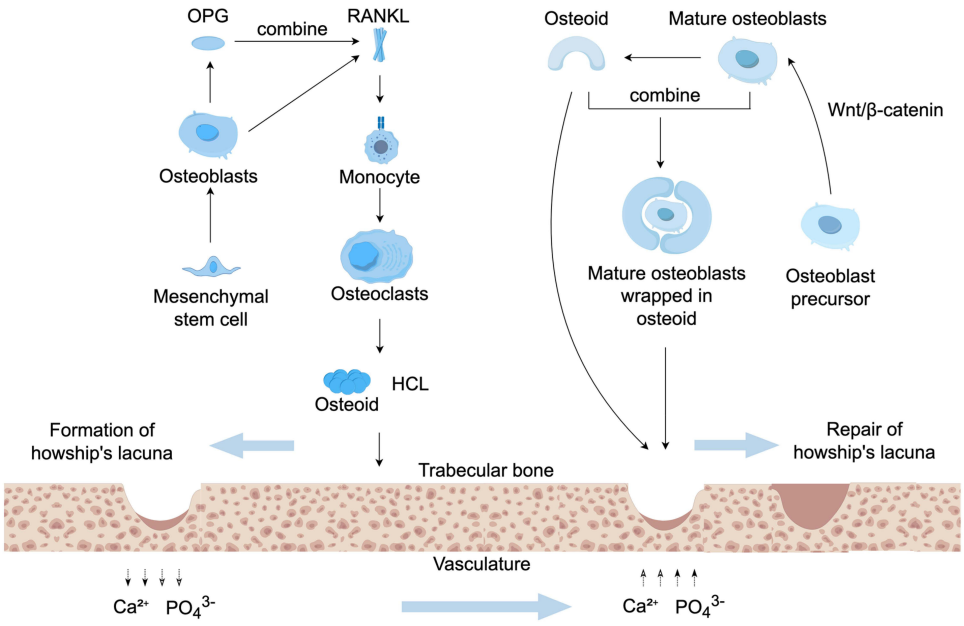

Figure 4 Osteoblasts play a crucial role in the mechanisms of bone repair (by Figdraw).

superfamily signaling, particularly BMPs which promote osteogenic commitment of BMSCs by activating transcription factors such as Osterix (Osx) and Runx2 to initiate osteoblast lineage specification,[28,29] while Hedgehog signaling promotes osteoblast differentiation by upregulating PTHrP and enhancing osteoblast proliferation and survival.[30] Additionally, FGF2 promotes the proliferation of BMSCs by activating the ERK/MAPK pathway.[31] Enhancing bone tissue regeneration by promoting the differentiation of BMSCs into osteoblasts is a key therapeutic strategy, as this process directly contributes to bone matrix synthesis and mineralization.

Osteoclast derived from hematopoietic stem cells (HSCs), play an equally critical role in bone remodeling by creating resorption pits that serve as biochemical and mechanical microenvironments for subsequent bone formation.[32] The process of bone repair is initiated when a bone defect occurs: Osteoblasts secrete the osteoclast differentiation factor (RANKL), which binds to mononuclear cells and induces their fusion into multinucleated osteoblasts.[33] The mechanism is RANK activation, triggering NF-κB and JNK signaling pathways.[34] Subsequently, the osteoclasts secrete lysosomal enzymes (primarily collagenase) and hydrochloric acid (HCl). The acidification is mediated by vacuolar H^+-ATPase and Cl^- channels in the osteoclast ruffled membrane.[35] Collagenase breaks down collagen fibers in the organic layer of the bone, forming resorption depressions known as Howship's lacunae. Simultaneously, HCl dissolves hydroxyapatite crystals in the inorganic matrix, converting them into calcium and phosphate ions that are released into the bloodstream.[36] Calcium and phosphate ions promote osteoblast mineralization by activating the calcium-sensing receptor (CaSR) and alkaline phosphatase (ALP), which hydrolyzes pyrophosphate to release phosphate. This process enhances hydroxyapatite deposition in the matrix. Wnt/β-catenin signaling upregulates Runx2/Osterix, stimulating mineralizing genes (BGLAP, COL1A1) while inhibiting PPARγ-mediated adipogenesis.[37,38] In addition, Wnt/β-catenin signaling not only initiates osteoblast differentiation but also drives terminal maturation by upregulating osteocalcin (OCN) and collagen synthesis through β-catenin/TCF4 transcriptional activation.[39]

The dynamic interplay between osteoclast-driven bone resorption and subsequent osteoblast-mediated formation establishes a core regulatory principle in skeletal renewal. This self-perpetuating cycle not only maintains mechanical competence but also regulates mineral exchange through phased tissue replacement.

To regulate this process, osteoblasts secrete osteoprotegerin (OPG), a molecule that specifically binds to RANKL and prevents its interaction with the RANKL receptor on the surface of monocyte-derived osteoclast precursors. Pro-inflammatory cytokines like TNF-α modulate this balance by enhancing the RANKL/OPG ratio during early repair phases.[28] This inhibition reduces osteoclast activity and ultimately contributes to osteoblast apoptosis.[40] As this stage

concludes, osteoblasts secrete collagen fiber-rich osteoids, which coat the osteoblasts and fill in Howship's lacunae left by osteoclast activity.

BMSCs-Material Interactions and Macrophage Polarization in Bone Regeneration: Anti-Inflammatory Repair and ROS Clearance

The functionality of osteoblasts in bone repair is intricately influenced by signals from surrounding niche cells, which guide stem cell responses based on an organism's needs. Under homeostatic conditions, the niche maintains osteoprogenitors in an undifferentiated state through cell-to-cell interactions and specific signaling. After a bone injury, changes in the niche environment initiate the differentiation of precursor cells into osteoblasts for tissue repair. Inflammatory cells, vascular endothelial cells (VEGF), and other components play critical roles in this process.[41]

Macrophages have a crucial role within osteogenesis, and both M1 and M2 macrophages are essential to make the inflammatory and remodeling phase have an adequate formation and recovery.[42]

When bone is damaged, inflammatory cells are activated, triggering a cascade of hematoma reactions. The first cells recruited are polymorphonuclear neutrophils (PMNs), Short-lived PMNs (<1 day) actively secrete chemokine-coordinated ligand 2 (CCL2), interleukin 6 (IL-6), etc, to recruit monocytes and other immune cells.[43] Subsequently, monocytes differentiate into macrophages, initially adopting a pro-inflammatory M1 phenotype under the influence of local signals such as interferon-γ (IFN-γ).[44] M1-type macrophages infiltrate the damaged area and promote the release of various chemokines such as transforming growth factor-alpha (TGF-α), IL-6, and Interleukin-1β (IL-1β). Biomaterial strategies actively modulate this phenotypic transition. For instance, β-TCP coatings activate the CaSR pathway to polarize macrophages toward the M2 phenotype, thereby upregulating bone morphogenetic protein-2 (BMP-2) expression and enhancing osteogenic differentiation of BMSCs.[45] Accelerating new bone formation by optimizing the adhesion and proliferation of BMSCs and osteoblasts on the material surface. This process synergizes with the β-TCP-mediated BMP-2 upregulation, as enhanced cell-material interactions directly promote osteogenic differentiation while sustaining growth factor availability. When applied to magnesium (Mg) scaffolds, β-TCP coatings synergistically reduce degradation rates, suppress toll-like receptor (TLR)-mediated proinflammatory signaling, and promote bone regeneration through sustained release of VEGF and BMP-2.[45] This targeted immunomodulation aligns with the natural progression of repair dynamics—as the repair progresses, M2-type macrophages, which produce anti-inflammatory cytokines, begin to dominate.

The establishment of alternatively activated macrophages (AAMs) involves coordinated regulation across cytokine signaling, epigenetic modifications, and metabolic reprogramming. T helper 2 (Th2) cell-derived interleukin-4 (IL-4) and interleukin-13 (IL-13) act as primary drivers of this process. Upon binding to their receptors, these cytokines initiate JAK kinase-mediated phosphorylation of STAT6. The activated STAT6 dimers subsequently translocate to nuclei where they directly bind promoters of characteristic M2 markers, including arginase 1 (ARG1), Fizz1, and Ym1/Ym2 - genetic signatures essential for maintaining AAM identity.[44] IL-10 further amplifies M2 polarization through a distinct mechanism. By activating the JAK1/TYK2-STAT3 cascade, this anti-inflammatory cytokine not only inhibits NF-κB-mediated pro-inflammatory responses but also establishes autoregulatory loops through simultaneous induction of IL-10 and TGF-β.[46] Upregulation of TGF-β effectively suppresses M1-associated markers, including inducible nitric oxide synthase (iNOS), through transcriptional repression mechanisms.[47] Emerging evidence highlights the pivotal role of metabolic sensors in this process. The PI3K-Akt-mTOR axis coordinates cellular energy status with transcriptional programs during AAM differentiation.[48] Intriguingly, metabolic byproducts like lactate directly influence chromatin states through histone h3 Lysine 18 lactylation (H3K18la), creating epigenetic memory for sustained M2 gene expression.[49] Non-coding RNAs, particularly lnc-BAZ2B and microRNA clusters (miR-375, miR-let-7),[50,51] further stabilize the M2 phenotype through post-transcriptional regulation of key signaling components.

M2-type macrophages secrete pro-tissue repair signaling molecules, including interleukin-10 (IL-10), transforming growth factor-β (TGF-β), and VEGF, which collectively recruit mesenchymal stem cells, promote neovascularization, and induce osteogenic differentiation of bone progenitor cells.[52]

Additionally, while low levels of ROS are essential for intracellular signaling and pathogen clearance, excessive production of reactive oxygen species (ROS) due to the disrupted ROS metabolism adversely affects the differentiation and resorption functions of osteoclasts, inducing osteoblast apoptosis and damaging cellular components such as proteins, DNA, lipids, and their membranes. These factors significantly hinder the process of bone repair.[53–55] Moreover, infections caused by pathogenic bacteria in the skeletal system disrupt bone repair through microenvironmental destabilization (fibrosis, osteolysis, ischemia) and systemic inflammatory cascades[56,57] Facilitating tissue repair by inducing the transition of M1-type macrophages to anti-inflammatory M2-type is critical to counteract these challenges. As described in biomaterial strategies (eg, β-TCP coatings), M2 polarization suppresses TLR-mediated proinflammatory signaling and enhances BMP-2/VEGF release. This phenotypic shift not only reduces infectious inflammation by secreting IL-10 and TGF-β but also indirectly mitigates ROS accumulation through the resolution of inflammatory cascades. By restoring microenvironmental stability, M2 dominance supports subsequent stages of bone regeneration.

Dual Structural-Molecular Strategy for Vascularized Microenvironment and Bone Healing

The formation of a vascular network during bone repair is not only crucial for attracting BMSCs but also relies on a pro-angiogenic microenvironment.[58] VEGF also facilitates the production of osteoinductive factors such as BMP-2 and TGF-β, which further enhance osteogenic differentiation and mineralization.[59] Specifically, CD31hiEmcnhi endothelial cells orchestrate osteogenesis through dual mechanisms: (1) direct secretion of angiocrine factors (eg, VEGF and platelet-derived growth factor-bb (PDGF-BB)), and (2) supporting pre-osteoclasts in PDGF-BB production, both of which converge to activate the Osterix/BMP2 signaling axis in osteoprogenitors.[60] Notably, recent studies revealed that Kindlin-2 regulates bone homeostasis by promoting Trim28-mediated ubiquitination degradation of Piezo1, thereby suppressing the calcium signaling-activated TGF-β/Runx2 axis and inhibiting endothelial-to-osteoblast conversion (EC-to-OSB).[61] Engineered scaffolds with interconnected porous structures facilitate nutrient diffusion and endothelial cell migration, while sustained release of VEGF mimics physiological angiogenesis. This dual strategy—structural support coupled with molecular signaling—ensures efficient oxygen and nutrient supply to osteoprogenitors, thereby preventing necrosis and supporting mineralization.

The mechanisms of bone repair can be summarized as follows: 1. Enhancing bone tissue regeneration by promoting the differentiation of BMSCs into osteoblasts. 2. Accelerating new bone formation by optimizing the adhesion and proliferation of BMSCs and osteoblasts on the material surface. 3. Ensuring effective delivery of nutrients and supporting bone healing by creating a favorable microenvironment conducive to neovascularization. 4. Facilitating tissue repair can be induced by inducing the transition of M1-type macrophages to anti-inflammatory M2-type, scavenging excess ROS and reducing infectious inflammation.

Biological Characterization of β-TCP

β-TCP is a calcium phosphate ceramic material with a rhombohedral crystal structure (space group R3c), chemically represented as β-$Ca_3(PO_4)_2$, exhibiting a Ca/P molar ratio of 1.5. Under physiological conditions, β-TCP demonstrates low solubility (approximately 0.0005 g/L at 25°C, with a solubility product log (Ksp) = −28.9, contributing to its cell-mediated resorption mechanism. However, the material exhibits inherent mechanical limitations, with theoretical tensile strength ranging between 1–10 GPa (approximately 1–10% of its theoretical Young's modulus of 110 GPa) and experimental values significantly lower due to ceramic brittleness.[62] β-TCP has been used clinically as a bone graft material for over a century.[63] Its composition closely resembles that of the inorganic layer of human cortical bone. Although β-TCP exhibits low solubility under physiological conditions, it undergoes progressive breakdown through osteoclast resorption. This process, primarily driven by cellular activity that acidifies the local environment, promotes the solubilization of β-TCP, releasing calcium and phosphate ions essential for osteoblast attachment, proliferation, and differentiation.[64] These ions also provide the inorganic components required for new bone formation.[65] Moreover, previous studies by Yuan et al demonstrated that β-TCP exhibits osteoinductive capacity comparable to autologous bone grafts in large animal models (canine and ovine), which may be attributed to its highly microporous structure, rapid calcium ion release, and protein adsorption capability that collectively

promote osteogenic differentiation of BMSCs.[66] Furthermore, a retrospective study by Lee et al revealed that the utilization of highly porous β-tricalcium phosphate (β-TCP) combined with bone marrow aspirate concentrate (BMAC) in midfoot joint arthrodesis resulted in a significantly higher union rate (91.5%, 43/47 joints) compared to the control group without β-TCP /BMAC application (76.2%, 32/42 joints), which may further validate the osteoinductive properties of β-TCP.[67] β-TCP achieves a superior balance between degradation and osteogenesis compared to hydroxyapatite (HA)—which exhibits limited bone regeneration due to dense, stoichiometric hydroxyapatite has a limited reactivity in vitro—and bioglass—hampered by brittleness and poor load-bearing capacity.[68,69] β-TCP maintains structural stability during early healing while progressively resorbing to match new bone formation.[62] Thereby avoiding HA's residual fragments and BG's premature collapse.

Modifying β-TCP's Mechanical Strength

Achieving appropriate compressive strength is critical for surgical success and long-term stability of the implants. It also aids in vascular reconstruction and facilitates the delivery of nutrients and oxygen, reducing cell loss and supporting normal tissue growth.[70]

To balance porosity and compressive strength, 3D printing technology has currently been employed to fabricate β-TCP scaffolds. Xu et al developed a light-cured β-TCP paste for Fused Deposition Modeling (FDM), successfully producing porous scaffolds[71] These scaffolds achieve compressive strengths of 16.53 and 10.42 MPa at porosities of 56.42% and 64.79%, respectively, meeting the required compressive strength range (4–12 MPa) of cancellous bone. Artificial polymers are frequently added to β-TCP composites to optimize mechanical properties and degradation rates. The composite design enabled pore formation as PGA degraded, partially compensating for mechanical strength loss through interaction with the newly formed bone tissue and the implant. Experimental results indicate that composite scaffolds fabricated with a 1:1 PCL-to-PGA ratio and containing 20 wt% of β-TCP are optimal for bone defect repair. A design that effectively leverages the markedly different degradation rates of PGA and PCL, while skillfully balancing porosity and compressive strength, has the potential to offer an innovative and practical solution to the challenges in related fields.

To address the brittleness of β-TCP materials, researchers have proposed effective solutions. For example, Umrath coated β-TCP scaffolds with three polylysine polymers (PDL-02, PDL-02a, and PDL-04) and compared the mechanical properties of β-TCP scaffolds before and after coating.[72] The results indicated that the PDL-04 coating significantly increased the toughness of the β-TCP scaffolds compared to the other coatings.

3D printing combined with synthetic polymers has also proven effective in bone tissue engineering. Wang et al fabricated polylactic acid (PLA)/nano-β-TCP composite scaffolds using FDM, demonstrating personalized porosity and exceptional osteogenic ability and biocompatibility, confirmed by animal model experiments on rabbit femoral defects.[73]

Similarly, PLA/β-TCP composite scaffolds were created using liquid crystal display (LCD) light-curing 3D printing technology.[74] The amount of β-TCP added was 0%, 10%, 20%, 30% and 35%. The gradual increase of β-TCP content increased compressive strength, reaching a peak of 52.1 MPa with 10% β-TCP, followed by a gradual decline at higher concentrations. These results showcase the optimization of the mechanical properties of the β-TCP, which provides important advances to the biomedical field.

Metal additives have further enhanced β-TCP properties. Zhou et al prepared a three-dimensional porous scaffold using polylactic acid-hydroxyacetic acid copolymerization (PLGA), β-TCP, and magnesium, through low-temperature deposition manufacturing (LTDM).[75] This composite has a high porosity of 63% and an interconnected microstructure with mechanical properties approximating those of cancellous bone. Xu successfully prepared β-TCP/titanium dioxide (TiO_2) porous ceramic scaffolds for the first time using three-dimensional gel printing and sintering technology.[76] The addition of 5 wt% TiO_2 significantly enhanced the compressive strength of the stent by up to 283%. According to their in vitro studies, this β-TCP/TiO_2 composite scaffold was non-toxic and demonstrated good biocompatibility. Other researchers have also addressed the brittleness of β-TCP materials by adding specific compounds. Ge and his team developed scaffolds using poly (1,8-octanediol-co-F127 citrate) (POFC), which has excellent hydrophilic properties, and β-TCP.[77] The POFC effectively mitigated the brittleness of the composite stent while maintaining its original pore structure.

Improvement of Degradation Rate

To effectively promote bone repair, the degradation rate of composite scaffolds should match the rate of new bone production. The pore-like network structure enhances the absorption and degradation of β-TCP. Although this material gradually dissolves during osteogenesis, the degradation rate of β-TCP scaffolds does not typically meet clinical needs. β-TCP has some biomechanical limitations. First, to prevent the collapse of nascent tissues, bone tissue engineering materials must withstand compressive loads. β-TCP, as a bioceramic, lacks sufficient mechanical strength to meet this requirement, rendering it prone to fracture or collapse.[78] Second, the rate of scaffold degradation must align with the rate of deposition of the mineralized tissue to ensure a gradual transition of mechanical support from the scaffold to the newly formed tissue.[79] Thus, controlling the degradation rate of β-TCP remains a challenge.

Formula modifications, such as sodium alginate-induced porosity, can enhance β-TCP degradation by creating interconnected pores that accelerate resorption. However, rat studies revealed acute inflammation (neutrophils/giant cells) around β-TCP/β-TCMP granules, potentially linked to residual alginate traces detected via FTIR. This underscores the importance of balancing degradation optimization with biocompatibility through rigorous purification.[80] Putri et al developed a β-TCP block featuring a bi-porous structure through the curing reaction of β-TCP particles.[81] This innovative material exhibited a fully interconnected network of macropores with uniformly distributed micropores along the walls surrounding the macropores. After four weeks of bone defect repair in the distal femur of rabbits using porous-TCP blocks, the treated region demonstrated higher bone resorption rates and greater new bone formation, highlighting its efficacy in promoting bone tissue regeneration. Seidenstuecker et al evaluated the compressive strength of β-TCP porous scaffolds enhanced with alginate dialdehyde (ADA)/gelatin using a Zwick Z005 universal testing machine.[82] The material degradation was assessed over 60 days in a Tris buffer solution at pH 7.4, following ISO EN 10993-14 standard. The results showed that the β-TCP porous scaffolds containing ADA/gelatin exhibited significant advantages in compressive strength and degradation rates compared to scaffolds without any added loading.

The addition of artificial polymers combined with 3D printing technology remains an effective strategy to improve the β-TCP degradation rate. Kumar et al created a PCL-PGA-β-TCP nonporous scaffold by incorporating varying ratios of Polycaprolactone (PCL), known for its mechanical strength, and polyglycolic acid (PGA), noted for its degradability (Figure 5).[16] Furthermore, Wu et al prepared scaffolds by mixing PCL with β-TCP in different ratios using FDM.[83] These scaffolds showed stable degradation characteristics and good osteogenic ability when the PCL-to-β-TCP mass ratios were 7:3, 6:4, and 5:5. Based on experimental observation in rats, bone tissue repair was successfully achieved after 16 weeks.

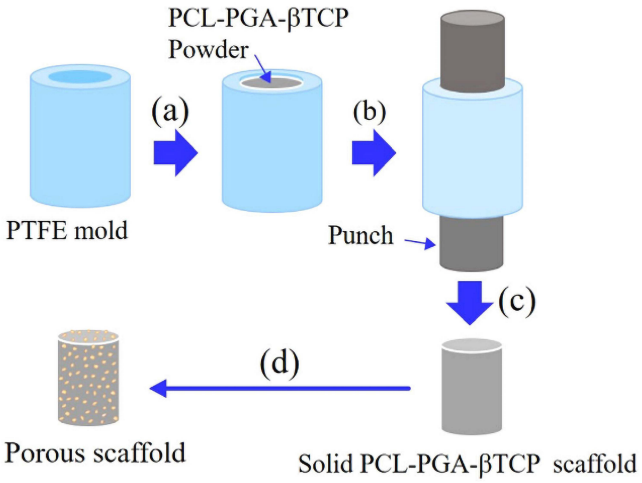

Figure 5 Schematic showing the fabrication of PCL-PGA-beta TCP scaffolds using compression molding of precursor PCL-PGA-beta TCP powder. (**a**) PCL-PGA-beta TCP composite powder was transferred to the cylindrical-shaped mold. To prepare the PCL-PGA-beta TCP powder, PCL, PGA, and beta TCP were mixed in HFIP, followed by drying at room temperature. The dried powder was treated with liquid nitrogen and then crushed into a fine powder. (**b**) Mold was heated to 150 C and samples was compressed to 50% of the initial height. (**c**) The samples were reheated to 150 C to relieve the stress generation due to compression, followed by cooling. (**d**) During the in vitro dissolution study in 1×PBS, faster degradation of PGA leads to the creation of a porous PCL scaffold. beta TCP, beta tricalcium phosphate; HFIP, 1,1,1,3,3,3-Hexafluoro-2-propanol; PCL, poly(caprolactone); PGA, poly(glycolic acid). Reproduced from Kumar A, Mir M, Aldulijan I, et al. Load-bearing biodegradable PCL-PGA-beta TCP scaffolds for bone tissue regeneration. J Biomed Mater Res B Appl Biomater. 2021;109(2):193–200. Copyright © 2020 Wiley Periodicals LLC.[16]

In another study, Zhu prepared composites using lactic acid-glycolic acid copolymer (PLGA) as the matrix and β-TCP as the inorganic filler via the melt blending method.[84] These composites were further processed to produce absorbable interface screws using injection molding. These screws were tested for in vitro degradation to identify the critical time point for the loss of mechanical properties. The results showed that the screws remained strong for 26 weeks, coinciding with the patient's wound-healing cycle. This study provided important reference data for the degradation characteristics of PLGA/β-TCP composites and laid the foundation for developing resorbable medical products based on such materials.

Furthermore, metal doping can modulate the rate of β-TCP degradation. Kim prepared iron-strontium co-doped β-TCP materials using an aqueous-phase co-precipitation technique and thoroughly investigated their in vitro degradation behavior.[85] Iron and strontium accelerated the degradation process on the surface of β-TCP, improving its reabsorption properties and providing enhanced degradation control due to the inherent magnetism of iron. The substitution of iron resulted in the formation of rough structures on the surface of the β-TCP samples, ranging from micrometers to sub-micrometers, according to cell adhesion experiments, which significantly enhanced cell adhesion and proliferation. The addition of growth factors can also enhance the absorption of β-TCP. Kakuta et al developed a cylindrical β-TCP material containing BMP-2 with porosities of 20.3% in the central macropores and 38.5% in the peripheral macropores.[86] This scaffold promoted β-TCP resorption by osteoclasts and the generation of new bone in a rabbit model with bilateral columnar bone defects in the distal femur.

To systematically compare the performance of β-TCP-based composite scaffolds, Table 1 summarizes key parameters such as porosity, compressive strength, degradation rate, and in vivo outcomes across representative studies. For instance, PLA/β-TCP scaffolds fabricated via LCD 3D printing achieved a compressive strength of 52.1 MPa with 10% β-TCP content, demonstrating superior mechanical properties compared to sintered β-TCP scaffolds.[74] Meanwhile, PLGA/β-TCP/Mg composites exhibited good degradation rates (60 days in vitro), highlighting the role of polymer-metal hybridization in balancing stability and resorption.[75]

Methods to Promote Bone Repair

Enhancement of Osteoinductivity

Osteoinductivity refers to the ability of a bone-replacement material to guide the differentiation of BMSCs into osteoblasts, thereby facilitating bone regeneration. Advances in modifying the spatial structure of β-TCP combined with artificial polymers have proven effective in this domain. For this instance, López-González and his team cultured adult bone marrow mesenchymal stem cells (ah-BM-MSCs) in vitro using a porous composite scaffold created by mixing β-TCP particles with PCL.[87] Mineralization assays and ALP activity demonstrated that this scaffold significantly promoted the expression of ossification-related genes. Similarly, Wang designed a multi-scale structural scaffold of PCL/β-TCP using FDM, which notably enhanced osteogenic differentiation of cells in osteoinduction studies.[88] Zheng further improved these results by adding calcium sulfate ($CaSO_4$) to PCL/β-TCP composites, which outperformed PCL scaffolds in inducing BMSC differentiation.[89] This improvement likely stems from its regulatory influence on the expression of genes related to bone metastasis.

The use of natural polymers to modify β-TCP has also yielded promising results. Luo et al combined the biocompatible gelatinized methacrylic acid (GelMA) with β-TCP, leveraging its superior biocompatibility to enhance BMSC attachment, proliferation, survival, and osteogenic differentiation.[90]

Researchers have also explored the integration of induction factors into bionic scaffolds to amplify bone tissue induction. To mimic the original femoral cortical bone structure, Lee constructed 3D-printed PCL/β-TCP scaffolds.[17] On these basic scaffolds, they applied Polydopamine (PDA), which has strong adhesive properties on diverse material surfaces, and used surface modification technology to effectively enhance the hydrophilicity and cell adhesion of the scaffolds. Furthermore, sustained release of BMP-2 was achieved by introducing alginate microbeads (AM) (Figure 6). In vitro experiments showed that the composite scaffold exhibited exceptional osteoinductive ability in both ALP, alizarin red S-staining (ARS), and quantitative real-time polymerase chain reaction (RT-qPCR) assays. Similarly, recent pre-clinical studies demonstrate that recombinant human BMP-7 (rhBMP-7) combined with nanometric hydroxyapatite-coated titanium implants significantly enhances new bone formation (55.3% vs 19.7% in over-instrumented sites),

Table 1 Comparative Performance of β-TCP Composite Scaffolds

Composite Scaffold Composition	Fabrication Method	Porosity (%)	Compressive Strength (MPa)	Degradation Period	Bioactivity	Cell Response	Animal Model Outcomes	References
β-TCP (microporous + BMP-2)	Sintering (pore control)	60	22	24 weeks	Microporosity↑TRAP+ cells, BMP-2↑osteogenesis	New bone↑ (Group C > B)	Rabbit femur: New bone growth (24 weeks)	[86]
PLA/β-TCP	LCD 3D printing	63	52.1 (10% β-TCP)	pH-dependent degradation (alkaline)	Alkaline pH↑mineralization	MC3T3-E1↑proliferation/ALP/OCN	Rabbit calvaria: Bone regeneration↑	[74]
POFC/β-TCP (Sr-loaded)	FFS-MDJ 3D printing	48	30–60 (modulus)	10 weeks (in vitro)	Sr↑osteogenesis/↓osteoclasts	rBMSCs↑mineralization/Col1	Osteoporotic bone: Density recovery↑	[77]
PCL-PGA-β-TCP	Compression molding	N/A	92 (50% strain)	PGA-dependent degradation	PGA↑porosity post-degradation	N/A	Load-bearing potential (untested)	[16]
PLGA/β-TCP/Mg	Low-temperature deposition	63	Similar to cancellous bone	60 days (TRIS buffer)	Mg↑bioactivity/ISO 10993-14 compliant	MC3T3-E1↑proliferation/Runx2	Rabbit calvaria: Bone bridging (8 weeks)	[75]
β-TCP + ADA-gelatin hydrogel	Flow-chamber loading	N/A	RMS ceramic: 931 → 1114 (post-loading)	60 days (TRIS buffer)	Non-toxic degradation↑protein adsorption	hDPSCs↑adhesion	N/A	[82]
Fe/Sr co-substituted β-TCP	Co-precipitation	N/A	Co-precipitation	21 days (TRIS-HCl)	Fe↑adhesion, Sr↑bone metabolism	hDPSCs↑adhesion/proliferation	N/A (magnetic hyperthermia potential)	[85]

Notes: 1. Symbols & Testing Standards: ↑: Indicates enhancement (eg, "BMP-2↑osteogenesis" = BMP-2 enhances osteogenesis); →: Denotes range/transition (eg, "931→1114" = RMS ceramic stress improvement range); N/A: Data unavailable or untested; Compressive strength: Values in parentheses indicate testing conditions (eg, "50% strain"); Degradation periods: "In vitro" labels specify lab testing; unspecified entries lack experimental context. 2. Technical Terminology: TRAP+ cells: Tartrate-resistant acid phosphatase-positive osteoclasts; ALP/OCN: Alkaline phosphatase (early osteogenic marker)/osteocalcin (late-stage bone formation marker); Runx2: Master transcription factor regulating osteoblast differentiation. 3. Fabrication Methods: LCD 3D printing: Liquid Crystal Display-based photopolymerization (±20μm precision); FFS-MDJ 3D printing: Fused Filament Fabrication with Multi-Dispenser Jets for multi-material composites; GA-dependent degradation: Degradation rate controlled by glycolic acid copolymerization ratio. 4. Additional Notes: pH-dependent degradation: Alkaline environments accelerate PLA/β-TCP composite degradation; Magnetic hyperthermia potential: Fe/Sr co-doped β-TCP requires experimental validation for external magnetic field responsiveness.

https://doi.org/10.2147/ORR.S525959

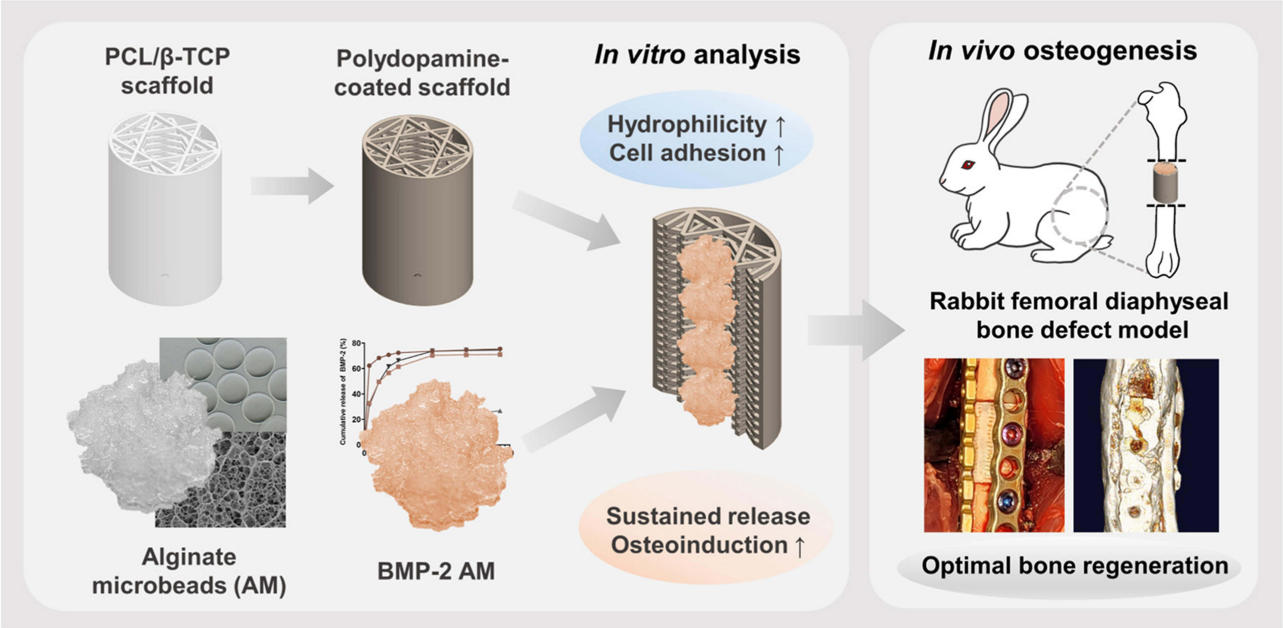

Figure 6 The idea and purpose of making a composite stent. Reproduced from Lee S, Kim JH, Kim YH, Hong J, Kim WK, Jin S, Kang BJ. Sustained BMP-2 delivery via alginate microbeads and polydopamine-coated 3D-Printed PCL/β-TCP scaffold enhances bone regeneration in long bone segmental defects. J Orthop Translat. 2024 Oct 2;49:11-22. © 2024 The Authors. This is an open access article under the CC BY-NC-ND license.[17]

particularly in challenging surgical scenarios where primary bone-implant contact is compromised, through rapid protein adsorption and osteoinductive activation.[91] These findings underscore the versatility of BMP family members: while BMP-2 excels in scaffold-based bone regeneration, BMP-7 shows unique efficacy in implant-osseointegration contexts.

Inspired by the bilayer structure of natural osteochondral tissue, Wang et al successfully developed an innovative bilayer osteochondral scaffold using 3D printing.[92] The two-layer scaffold consists of a lower layer that mimics the porous subchondral bone using a bone peptide/β-tricalcium phosphate/poly (lactic-co-glycolic acid) water-in-oil composite emulsion material, while the upper layer is a poly(D, L-lactic-co-trimethylene carbonate) water-in-oil emulsion that mimics the natural cartilage structure. The researchers also added a type I collagen hydrogel enriched with transforming growth factor-β1 (TGF-β1), which enhances the upper layer. In vitro experiments showed that rat BMSCs exhibited extremely high survival rates and significant proliferative activity, both in the subchondral and cartilaginous layers. Metal doping in β-TCP shows concentration-dependent osteogenic effects. Yassuda et al demonstrated that magnesium-doped β-TCP (β-TCMP, Ca/Mg=0.15) exhibited 36% lower resorption and reduced new bone formation compared to pure β-TCP in rat dental sockets after 42 days ($p<0.001$). Mechanistically, β-TCP elevated serum PTH levels (8.5 vs 5 pg/mL) and RANK-L/OPG ratios (0.32 vs 0.18 at 21 days), enhancing osteoclast activity.[93] Saito et al developed a bioscaffold based on β-TCP with 1.0 wt% magnesium oxide (MgO), zinc oxide (ZnO), strontium oxide (SrO), and silicon dioxide (SiO_2).[94] To assess the effect of these composites on cell behavior, BMSCs from 7-week-old male rats were cultured on these scaffolds for two weeks under standard conditions. ALP activity and gene expression involved in osteogenic differentiation were examined. All scaffolds were implanted into the subcutaneous tissue of rats and removed after seven weeks of continuous observation to further analyze their in vivo biocompatibility and osteogenic properties. MgO samples showed lower levels of calcium release and higher mRNA expression of osteogenesis-related markers compared to pure β-TCP scaffolds. In vivo experiments indicated that MgO scaffolds not only showed higher ALP activity but also significantly increased transcript levels of BMP-2 and VEGF, as determined by real-time fluorescence quantitative PCR. Micro-computed tomography (micro-CT) also revealed that bone formation was best in the MgO group.

Drug loading in composite scaffolds is a common strategy for effectively enhancing their osteoinductive properties. For instance, Gu utilized *Ti3C2Tx* (MXene) to modify poly (lactic-co-glycolic acid)/β-tricalcium phosphate/ Icariin (PLGA/β-TCP/ICT) porous scaffolds (PTI).[95] The TIM-modified composite scaffolds maintained their original properties and promoted cell proliferation and osteogenic differentiation through near-infrared (NIR) radiation on ICT. The release

of ICT can be effectively promoted, further enhancing the biological activity and therapeutic effect of the scaffold by modulating NIR radiation.

As a unique bioceramic, bioglass has received considerable attention from researchers due to its ability to promote bone regeneration through ion release. Westhauser found that the addition of 45S5 BG particles to β-TCP promoted earlier differentiation of BMSCs into osteoblasts without adversely affecting cell viability.[96] Kazemi, on the other hand, prepared porous nanoscale scaffolds by using cesium to replace calcium β-phosphate and BG, and found that strontium-β-calcium phosphate (Sr-TCP) exhibited optimal osteoinductive properties when the ratio of strontium-β-calcium phosphate (Sr-TCP) to BAG was 1:1.[97] Other researchers have focused on modifying BMSC genes. Increasing the level of miR-136-5p significantly enhances the osteogenic differentiation ability of BMSCs, as discovered by Duan et al. Based on this important finding, they constructed a rabbit distal femur defect model and combined miR-136-5p-modified BMSCs with β-TCP biomaterials to create composite scaffolds for implantation into the defect site.[98] The researchers performed a detailed assessment of the effectiveness of bone defect repair using micro-CT imaging and histological HE staining. The results showed that this scaffold material could effectively promote the transformation of BMSCs into mature osteoblasts and significantly accelerate the repair process of bone defect areas.

Recently, electrostatically spun nanofiber scaffolds have gradually become popular materials in the field of bone tissue engineering owing to their large-scale production capacity, low toxicity, flexible adjustment, and fine-tuning of scaffold properties by chemical modification[99–101] Ramanathan developed an electrospun cotton-like fiber composite of β-TCP and poly(lactic acid)/poly(hydroxyl colic acid) (PLLA/PGA), and then conducted a comparative study of the osteoinductive properties of this composite with those of pure β-TCP through a rat model of mandibular defects.[102]

The results showed that the β-TCP/PLLA/PGA composites exhibited a significant increase in osteoblast aggregation at both the early and late stages of implantation, demonstrating superior performance in osteoinduction. Mahmoud prepared a novel nanoscale GelMA/PCL photocrosslinked porous composite fiber membrane loaded with β-TCP gelatin using electrostatic spinning technology.[103] Compared with PCL and GelMA/PCL composites alone, this GelMA/PCL-β-TCP membrane significantly promoted adhesion, proliferation, mineralization, and expression of osteogenic-related genes in alveolar BMSCs. Importantly, the electrospun GelMA/PCL/β-TCP membrane balances nanofibrous guidance (500–1500 nm fiber diameter) with a high modulus (117.9 MPa), attributes critical for periodontal tissue regeneration (rat calvarial model), yet it faces challenges in synchronizing degradation rates with osteogenesis.

Furthermore, new advances in electrospinning may enable innovative designs of β-TCP-based scaffolds by leveraging nanofiber architectures for bone regeneration. The technique may provide a precise encapsulation of β-TCP into compartmentalized nanostructures (eg, core-shell or Janus configurations), optimizing both mechanical reinforcement and bioactive delivery.[104] For instance, coaxial electrospun PCL nanofibers incorporating calcium phosphate ceramics demonstrate the feasibility of adapting β-TCP into similar strategies, combining osteoconductivity with polymer flexibility.[105] Janus electrosprayed systems further exemplify dual-functional designs, where spatial segregation of hydrophobic/hydrophilic components could inspire β-TCP/polymer blends coupled with growth factor reservoir.[106] In summary, the integration of β-TCP with electrospun nanofiber systems (eg, through Janus structures or core-shell encapsulation) offers novel insight for advancing bone regeneration efficacy and hierarchically functionalized bone scaffold design.

Strengthening Osteogenesis

Osteogenesis involves the activity of osteoblasts or BMSCs within composite implantable materials. These materials enhance cell adhesion and proliferation, promoting the formation of new bone tissue in suitable biological environments.

The incorporation of synthetic polymers into β-TCP is becoming a dominant strategy to enhance the osteogenic effect. For example, Zheng et al prepared PTMC/PCL/TCP composites, consisting of poly (trimethylene carbonate), poly (ε-caprolactone), and β-TCP using bio-3D printing technology.[107] They implanted the scaffolds into rat thigh bone defects after planting osteoblasts C3T3-E1 and rBMSCs, evaluated bone repair performance, cytotoxicity, and cell proliferation. The results showed that the scaffolds significantly promoted the proliferation of osteoblastic MC3T3-E1 cells and rBMSCs, while exhibiting low cytotoxicity and excellent biocompatibility. The combination of β-TCP with natural polymers such as natural rubber latex membrane (NRL) has shown synergistic osteoinductive effects. Giovanetti

et al found that NRL-β-TCP membranes not only supported MC3T3 preosteoblast adhesion but also upregulated ALP activity by 3.49-fold compared to controls, indicating enhanced osteogenic differentiation.[108]

Additionally, the incorporation of coatings that enhance osteoconductivity through synthetic polymers has attracted considerable attention from researchers. Yuan et al coated nanoscale demineralized bone matrix (DBM) with enhanced osteoconductive properties onto the surface of 3D-printed PCL/β-TCP scaffolds using FDM.[109] Mouse MC3T3 cells exhibited higher viability on nano DBM-coated PCL/β-TCP scaffolds compared to non-coated ones. In vivo experimental results showed that nano DBM-coated PCL/β-TCP scaffolds were superior to untreated PCL/β-TCP scaffolds in terms of new bone tissue growth. This result proved that nano DBM-coating could significantly enhance the performance of PCL/β-TCP scaffolds in terms of adhesion, proliferation, and activity. In a different study, Lu generated a functional molybdenum disulfide (MoS_2)/PDA/-BMP 2-insulin-like growth factor-1 (IGF-1) coating on a β-TCP scaffold and analyzed the outcome of in vitro osteogenesis.[110] The scaffold could significantly promote adhesion, expansion, and proliferation of BMSCs. More notably, the MPBI@β-TCP scaffold displayed outstanding photothermal conversion ability to effectively kill osteosarcoma MG-63 cells under NIR light conditions. This finding has potential applications in the field of bone defect tumors.

Adjusting the three-dimensional structure of the scaffolds also has the potential to improve their osteoconductive properties. To mimic the porous structure of natural bone, Qianjiang et al, developed PCL/β-TCP composite scaffolds with different pore sizes using 3D printing technology.[111] The scaffolds with a 2.5 mm pore size possessed excellent mechanical properties, cytocompatibility, and effectively promoted cell proliferation and adhesion. Additionally, these scaffolds were particularly effective in promoting new bone formation in rat in vivo experiments. Li et al, on the other hand, produced a hydroxyapatite/β-tricalcium phosphate/sericin (HA/β-TCP/SF) composite scaffold with both macroporous and microporous structures, and inoculated mouse MC3T3-E1 onto the scaffold.[112] The adhesion and proliferation of MC3T3-E1 cells on the composite scaffolds significantly increased, as shown by methyl thiazolyl tetrazolium colorimetry (MTT) assay, scanning electron microscopy (SEM), and hematoxylin-eosin (HE) staining. Furthermore, application in a rabbit tibial defect model indicated that composite scaffold implantation promoted new bone formation and significantly increased bone volume fraction, demonstrating the efficient performance of the scaffold in promoting osteogenesis.

Magnesium ions can effectively promote osteoblast activity by accelerating proliferation while inhibiting the osteolytic effect of osteoclasts. Thus, they are frequently added to scaffolding materials to enhance their bone growth ability. Gu et al prepared a series of magnesium-doped β-TCP scaffolds by applying LDM and sintering technology; human BMSCs and human umbilical vein endothelial cells (HUVECs) were cultured in the extract of the scaffolds.[113] Both cell types exhibited excellent proliferation rates, good cell morphology, and high cell viability, confirming the potential of magnesium-doped β-TCP scaffolds to promote osteogenesis and angiogenesis.

Furthermore, it has been reported that the role of Cu^{2+}, Si^{4+}, and Sr^{2+} ions are crucial in osteogenesis.[114] Based on this finding, Xu and his team produced a series of 3D-printed strontium copper tetra silicate/β-tricalcium phosphate (Wessel site $[SrCuSi_4O_{10}]/Ca_3(PO_4)_2$, or WES-TCP for short) composite scaffolds using different mass ratios.[115] Compared with pure β-TCP stents, this series of composite scaffolds achieved an effective increment in ion release and optimized mechanical properties. Particularly, the mechanical strength of WES-TCP was significantly enhanced when WES was 2 wt%. Moreover, the team evaluated the bioactivity of the composite in a rabbit cartilage defect model to determine its promotional effect on the proliferation of rabbit BMSCs and their expression of osteogenesis-related genes. The results showed that the proliferation of rabbit BMSCs on WES-TCP scaffolds was significantly increased compared to that on a pure β-TCP scaffold. Among these, the 2 wt% scaffold performed the best, with maximized proliferation efficiency and the highest level of osteogenic gene expression. These results confirm that 2 wt% WES-TCP possesses high compressive strength and effectively promotes the proliferation and differentiation of rabbit BMSCs, contributing positively to the regeneration of rabbit cartilage tissue.

Other scholars have utilized a screen-rich-combine circulating system (SECCS) to enhance osteogenesis. Chu et al evaluated the effect of SECCS-treated MSCs combined with β-TCP and filled with a titanium scaffold through a goat distal lateral femur half model.[116] The scaffold was compared with two control groups: a pure β-TCP scaffold and an

unfilled titanium scaffold. The SECCS-treated bone marrow BMSCs attached firmly to the scaffold, demonstrating significant proliferative capacity. Moreover, the new bone tissue growth area was significantly larger.

Enhancing Osteoconductivity

Osteoconductivity describes the ability of bone graft materials to provide a structural framework supporting blood vessels and new bone growth, thereby facilitating effective bone regeneration.

Conventional 3D-printed bio ceramic scaffolds often feature solid structures with low porosity, which restrict angiogenesis and bone tissue regeneration. To address this limitation, Tian et al constructed a β-TCP bioceramic scaffold with a hollow tubular configuration.[117] By fine-tuning the parameters of the hollow tubes, the team optimized the scaffold's physicochemical properties, resulting in improved early angiogenesis and superior late-stage bone formation in vivo, compared to traditional solid scaffolds. Similarly, Toda investigated nanocomposites comprising β-TCP, micron-sized HA, and poly-D/L-lactic acid (PDLLA) as bone graft substitutes in a critical bone defect in the lateral right mandible of 10-week-old rats.[118] Although micro-CT results showed that pure β-TCP had the highest bone density and bone volume/total volume, immunohistochemical analyses demonstrated that β-TCP/HA/PDLLA showed a superior ability to promote osteogenesis, especially in the early stages of the bone healing process. These findings confirm that this novel nanocomposite has good osteoconductivity and is an ideal choice for bone graft replacement materials in maxillofacial reconstructive surgery.

To further improve the osteoconductive efficacy of composite stents, 3D printing technology is widely used. Feng et al developed hierarchical porous scaffolds with connected macropores (~400 μm) and two types of micropores (spherical and fibrous).[119] These scaffolds were prepared by combining Direct Ink Writing (DIW) with a precisely controlled structure using the sacrificial template method. It was found that scaffolds containing highly connected fibrous micropores notably strengthened the adhesive properties of mouse BMSCs and HUVECs, compared to scaffolds containing only spherical micropores. This hierarchically structured scaffold with fibrous micropores could significantly promote bone repair in further in vivo implantation experiments. Wu and his team, on the other hand, fabricated a porous β-TCP/PCL composite scaffold with a gradient structure by combining DLP with a vacuum impregnation process.[120] The scaffold played an important role in promoting bone tissue regeneration and accelerating vascularization via its adjustable tapering properties and interconnected 3D network structure.

Various bionic structures have gradually become the focus of current research owing to the rapid development of 3D printing technology. Zhou et al presented a customized large porous β-TCP scaffold with a biomimetic vascular structure, which significantly optimized the overall vascular distribution by embedding the femoral-axial vascular bundle.[121] Compared with traditional β-TCP scaffolds, this new multichannel β-TCP scaffold was able to generate adequate vascular networks and bone-like tissues inside its porous structure after four weeks of implantation. Notably, the multi-channeled β-TCP scaffold, while prioritizing vascular integration (65.5% porosity) and rhBMP-2-mediated osteoinduction for mandibular reconstruction (in rabbit models), exhibits limited compressive strength (2.9–3.7 MPa) in load-bearing contexts. On the other hand, Zhang et al drew inspiration from the sandwich structure of the cranium and successfully developed two flat bone-mimetic β-TCP bioceramic scaffolds, Gyr-Comp and Gyr-Tub, using 3D printing.[18] The Gyr-Comp scaffold features two compact outer layer designs customized to match the low porosity characteristics of the flat bone outer table, while the Gyr-Tub scaffold has a tubular pore structure in the outer layer designed to accurately mimic Haversian and Ossmann's tubes in the external bone plate (Figure 7). To verify the effects of these bionic scaffolds on angiogenesis and osteogenesis, they constructed a rabbit cranial bone defect model and used CCK-8 assay, tubule formation assay, calcein-acetoxymethyl staining, mRNA expression of angiogenic genes, and immunofluorescence staining of CD31 to analyze the material. The results showed that these two novel scaffolds have obvious advantages in promoting cell proliferation in vitro, accelerating the rate of osteogenic differentiation, and improving the efficiency of angiogenesis compared to conventional cross-hatched structural scaffolds.

Some scholars have utilized supercritical carbon dioxide foaming in this field. Pitkänen et al successfully developed a β-TCP/poly(lactic-co-ε-caprolactone) (PLCL) bone composite with high-strength elasticity, suitable porosity, and biodegradable properties through a non-toxic, low-cost supercritical carbon dioxide foaming.[122] Human adipose stem cell differentiation into osteoblasts was detected using in vivo alkaline phosphatase activity, alizarin red staining, soluble

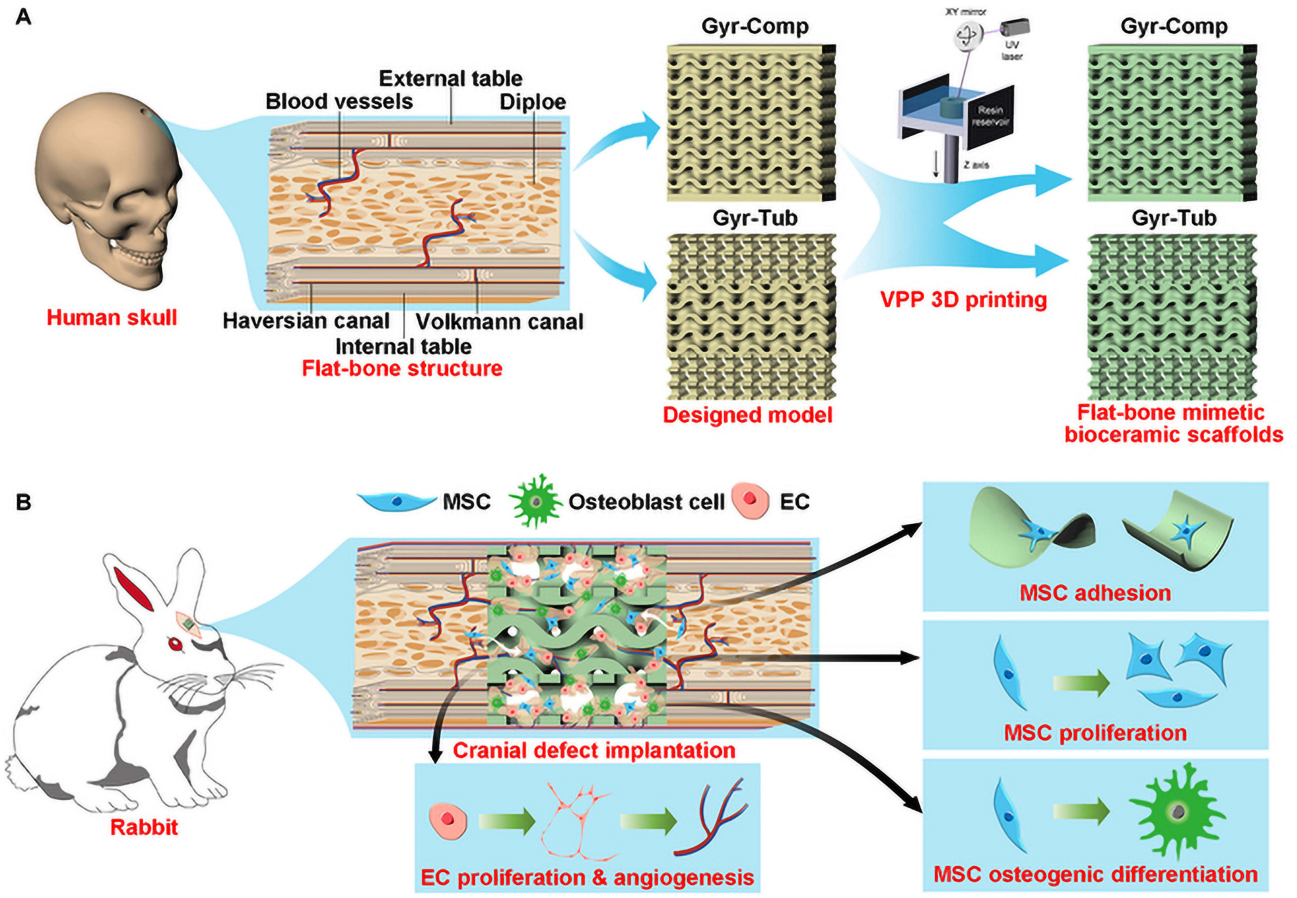

Figure 7 Schematic illustration of the design and bone regeneration potential of the flat-bone-mimetic bioceramic scaffolds. (**A**) The scaffolds are inspired by the sandwich structure of flat bone of craniums. (**B**) The scaffolds can provide a biomimetic structural environment to promote osteogenesis and angiogenesis. UV, ultraviolet. MSC, mesenchymal stromal cell; EC, endothelial cell. Reproduced from Yihang Zhang, Fupo He, Qiang Zhang, Haotian Lu, Shengtao Yan, Xuetao Shi. 3D-Printed Flat-Bone-Mimetic Bioceramic Scaffolds for Cranial Restoration. Research. 2023;6:0255. Copyright © 2023 Yihang Zhanget al. Exclusive licensee Science and Technology Review Publishing House. No claim to original U.S. Government Works. Distributed under a CreativeCommons Attribution License 4.0(CC BY 4.0).[18]

collagen analysis, immunocytochemical staining, and qRT-PCR. Additionally, in vitro experiments showed a remarkable mineralized collagen matrix after hASCs were cultured on this composite material for 21 days. The results indicate that this composite material possesses good osteoconductive and osteoinductive properties.

Metal doping is another effective method for improving osteoconductive properties in composites. Based on the key role of magnesium in bone metabolism, Qi et al adopted DLP printing technology to prepare β-TCP scaffolds containing varying concentrations of MgO.[123] The addition of magnesium to β-TCP scaffolds not only promoted the vascularized differentiation of endothelial progenitor cells (EPCs) but also enhanced the osteogenic differentiation of BMSCs through in vitro assays. Prabakaran et al fabricated a zinc-enriched calcium phosphate composite incorporating plant-derived antimicrobial agents that demonstrated 90% cell proliferation of MG-63 osteoblasts at optimized concentrations, significantly outperforming conventional treatments (45% cell viability with cisplatin-treated control group).[124]

Furthermore, the incorporation of proangiogenic drugs has interested researchers. Cheng used low-temperature rapid prototyping (LT-RP) technology to incorporate cucurbitacin B (CuB) into a biomaterial scaffold (PT/CuB) composed of biodegradable PLGA and β-TCP.[125] The scaffold promoted angiogenesis and accelerated the bone regeneration process in a rat fibula defect model. Further studies revealed that CuB effectively exerted its pro-angiogenic effect by activating vascular endothelial growth factor receptor 2 (VEGFR-2) and its associated signaling pathways.

Regulation of Inflammatory Responses

One key strategy for effective bone tissue regeneration is promoting the transition from the inflammatory response to tissue regeneration by promptly directing macrophages from M1 to M2 type. Based on this, Li designed a 1 wt% zinc

porous bionic scaffold (PTZ) that could continuously release a safe dose of zinc ions during 16 weeks by introducing zinc submicron particles into PLGA/β-TCP composites and applying LT-RP.[19] It was confirmed that the PTZ scaffolds could effectively promote osteogenesis and the transition of M1-type macrophages into M2, potentially related to the effect of Wnt/β-catenin and p38 MAPK/NFκB. Mechanistically, zinc ions activate Runx2 through the Wnt/β-catenin pathway, upregulating the expression of osteogenic genes (osteopontin (OPN), OCN) and enhancing mineralization through ectonucleotide pyrophosphatase/phosphodiesterase 1 (ENPP1) and high temperature requirement A1 (HTRA1). At the same time, zinc ions activate P38 MAPK, up-regulate connective tissue growth factor (CCN2) and IL-10, promote the polarization of M2 macrophages, and down-regulate TNF-α, interleukin-1 receptor antagonist (IL1RN), and eukaryotic translation initiation factor 2-alpha kinase 2 (EIF2AK2) while inhibiting the M1 phenotype. Furthermore, ALP staining (Figure 8a), ARS (Figure 8b), and RT-qPCR analyses (Figure 8c and d) revealed that PTZ scaffolds have improved osteogenic mineralization potential.

Enhancing the anti-inflammatory and osteogenic properties of β-TCP composite scaffolds by incorporating zinc submicron particles opens up new avenues for future clinical treatment of bone defects. Cao et al produced scaffolds with

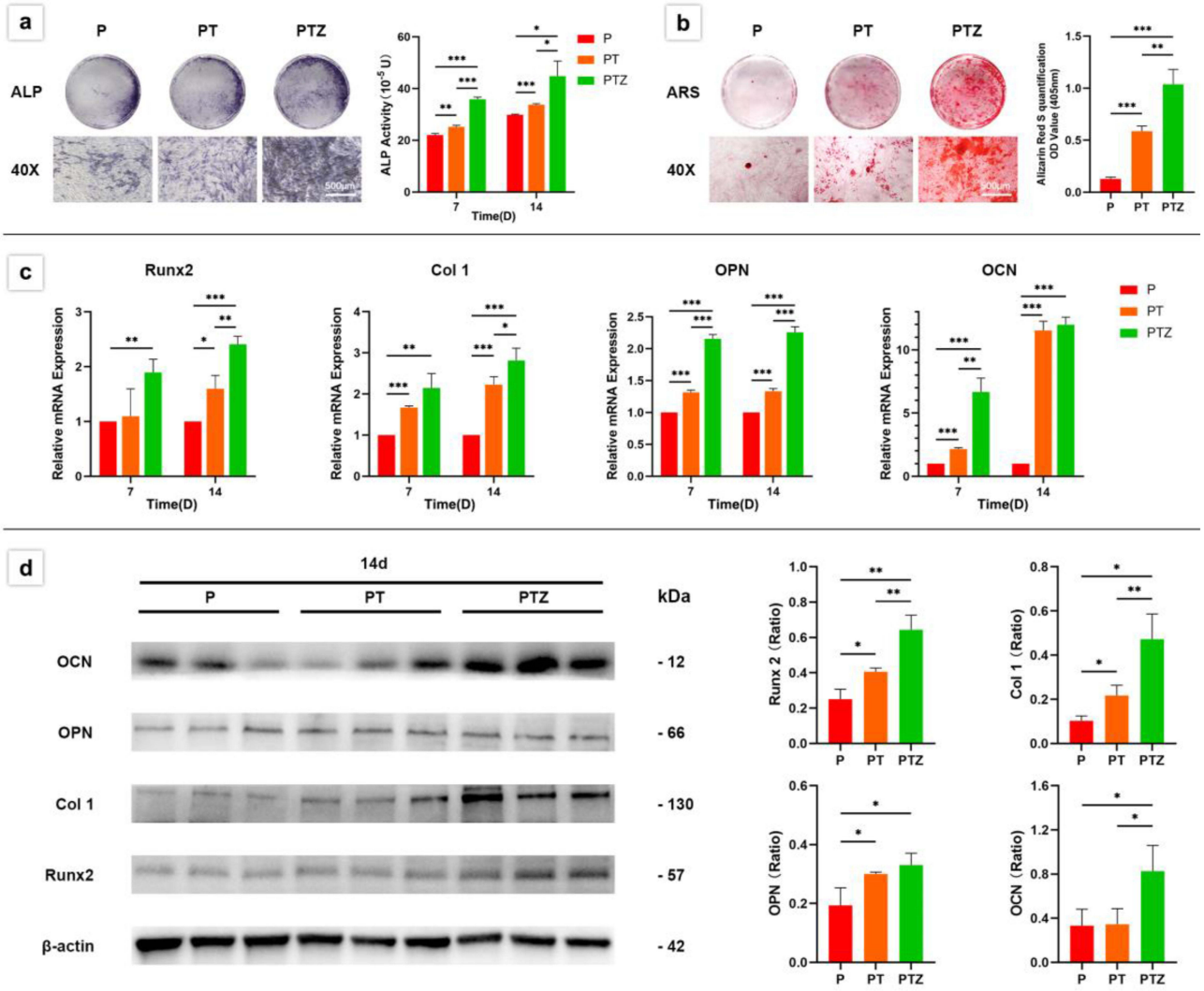

Figure 8 Steogenic differentiation ability of BMSCs co-cultured with three groups of scaffolds. (**a**) A quantitative analysis was performed after ALP staining at 7th and 14th day. (**b**) Calcium deposits were stained with alizarin red S and quantitatively analyzed after 21 days of culture. (**c**) The expression levels of Runx2, Col I, OPN and OCN were analyzed by RT-qPCR after 7 and 14 days. (**d**) The expression levels and quantitative analysis of Runx2, Col I, OPN, and OCN proteins detected by WB after 14 days. β-Actin was used as a protein loading control. (*p < 0.05, **p < 0.01, ***p < 0.001). Reproduced from $^{2+}$ in 3D-printed PLGA/β-TCP/Zn scaffolds for bone defect repair by improving osteoinductive and anti-inflammatory properties. Bioact Mater. 2022 Dec 31;24:361-375. © 2022 The Authors. CC BY-NC-ND license.[19]

coatings by encapsulating sphingosine 1-phosphate (S1P) on β-TCP scaffolds.[126] The scaffolds exhibited excellent immunomodulatory properties on macrophages and promoted the conversion of M1 macrophages into M2, while enhancing osteogenic differentiation of bone marrow stromal cells in rats. In a different study, Hu et al developed a bionic cancellous bone scaffold consisting of α/β-TCP with gelatin retained as the organic phase and a metal-polyphenol network structure containing tea polyphenol-magnesium (TP-Mg) nanoparticles embedded through 3D printing technology.[127] This scaffold promoted the conversion of macrophages from an M1 pro-inflammatory to an M2 anti-inflammatory phenotype with significant inhibitory effects on S. aureus. Moreover, the composite exhibited excellent bone-enhancement properties due to the synergistic effects between magnesium and calcium ions. The resulting 3D-printed porous scaffold (α-TCP/β-TCP/TP-Mg) further demonstrates a compressive strength exceeding 100 MPa and integrates dual antibacterial and anti-inflammatory functionalities, specifically designed to address infected weight-bearing bone defects.

Abnormally elevated ROS levels are the key factors hindering bone repair, and scavenging ROS by β-TCP modification has become an important strategy to promote bone repair. Huang et al found that Ti3C2-based materials exhibited excellent ROS scavenging ability, biocompatibility, and NIR photothermal conversion efficiency due to their inherent Ti-C redox activity centers.[128] In contrast, Zn and Sr ions have been shown to possess anti-inflammatory regulatory functions. This research team performed an innovative modification of a conventional β-TCP scaffold by employing thin-layer MXene-Ti3C2 modification and Zn2+/Sr2+ ion substitution. The composite scaffold not only has the ability to scavenge ROS but also enhances pro-inflammatory responses by promoting the M1-to-M2-type conversion, further accelerating the process of inflammatory regression. Gradual degradation of the 3D scaffolds and the sustained release of Zn2+ and Sr2+ ions helped maintain a favorable reparative immune microenvironment dominated by M2-type macrophages, effectively promoting the bone healing process. Mechanistically, Zinc ions inhibit the NLRP3 inflammasome and reduce the secretion of IL-1β. On the other hand, strontium ions activate CaSR, upregulating the expression of IL-10, and jointly assist in the polarization of M2 macrophages. On a similar note, Qian et al prepared a modified artificial periosteal material, β-TCP/MnO_2/PCL (β-TMP), with the function of catalyzing the decomposition of hydrogen peroxide (H_2O_2) by using electrostatic spinning technology.[129] The material effectively reduced intracellular ROS levels and enhanced osteogenic differentiation-promoting effects on BMSCs and MG-63 cells.

Loading antibiotic drugs onto β-TCP is used to address inflammation caused by infected bone defects. Qiu et al produced microspheres of vancomycin hydrochloride (Van) with poly (lactic acid)-poly (glycolic acid) (PLGA) using a double emulsion method and successfully integrated them into β-TCP scaffolds (CPSFs) by electrostatic action and physical cross-linking techniques.[130] CPSFs exhibited superior histocompatibility, biocompatibility, and sustained release of vancomycin, based on the results of X-ray imaging, micro-CT scanning, and histopathological analysis of rabbit models. This composite has potential clinical applications for treating localized infected bone defects. In a different study, Xu et al loaded metformin (MET) onto a composite scaffold consisting of β-TCP, chitosan (CTS), and mesoporous silica (SBA-15), and implanted it into the region of alveolar bone defects in rats with periodontitis.[131] This composite scaffold effectively promoted alveolar bone regeneration, as confirmed by micro-CT scanning and histological analyses after 12 weeks. The scaffold also efficiently activated the Wnt/β-catenin signaling pathway, exhibiting excellent antimicrobial activity. The acids that degrade PLGA may lead to inflammatory reactions and acidification of the tissues around the implantation site. However, PLGA is widely used in bone tissue engineering. To solve this problem, a PLGA/β-TCP/Mg(OH)2 nanocomposite scaffold (TCP/MH) modified by twin-screw extrusion was developed by Go and his team. This composite scaffold effectively suppressed the inflammatory response and facilitated the bone defect repair process, as demonstrated by the results of the rat humeral defect model.[132] The multifunctional synergy of β-TCP composites is critical for addressing complex bone repair requirements. As shown in Table 2, scaffolds such as β-TCP /MnO_2/PCL not only enhanced osteogenic activity but also promoted angiogenesis and suppressed inflammation. For example, MnO_2 integration catalyzed ROS decomposition.[129] While PLGA/β-TCP/Zn sustained Zn ion release modulates Wnt/β-catenin pathway and accelerated M1-to-M2 macrophage polarization, illustrating how ionic modulation can synergistically enhance bone regeneration.[19] Additionally, systematic evaluation of the control mechanisms exerted by different fabrication techniques on scaffold properties is critical. Table 3 summarizes that these processes exhibit notable differences in pore topology design, degradation kinetics matching, and mechanical strength optimization, which

https://doi.org/10.2147/ORR.S525959

Table 2 Osteogenic-Angiogenic-Anti-Inflammatory Synergy in β-TCP Composite Scaffolds

Composite Scaffold Composition	Osteoconductivity (ALP Activity)	Angiogenesis	Inflammation Regulation	Mechanisms	Statistical Data & Significance	References
PLGA/β-TCP + 1 wt% Zn	ALP activity increased by 2.3 times (14 days).	N/A	Accelerated M1→M2 polarization (IL-10 ↑40%)	Sustained Zn^{2+} release modulates Wnt/β-catenin pathway	Compressive strength: 2.89 ±0.03 MPa ($p<0.05$)	[19]
β-TCP + Ti3C2 MXene + Zn^{2+}/Sr^{2+}	ALP activity increased by 1.5 times (21 days).	CD31 expression ↑1.8-fold	TNF-α↓30%	NIR photothermal synergy with ion release	ROS scavenging rate: 82% ($p<0.01$)	[128]
50Sr-TCP/50BG	ALP activity is 1.8 times higher than pure beta-TCP (7 days).	Vascular density ↑ 35% (MT staining)	N/A	Sr^{2+}/Si^{4+} co-activation promotes collagen deposition	New bone area: 15.2 ±1.8 mm^2 ($p<0.01$)	[97]
PCL/β-TCP + BMP-2 microsphere	ALP activity increased by 2.5 times (21 days)	55% ↑ neovascularization (via μCT analysis)	M2 macrophages ↑ 60%	PDA coating enhances sustained BMP-2 release (85% release over 28 days)	Bone volume fraction: 42.3 ±3.1% ($p<0.001$)	[17]
β-TCP + 3 wt% MgO	ALP activity increased by 2.1 times (14 days)	CD31+ area ↑48%	ROS↓60%	Mg^{2+} activates PI3K/AKT pathway	Compressive strength: 4.2 ±0.3 MPa ($p<0.05$)	[123]
β-TCP/MnO2/PCL (0.1%)	ALP activity increased by 2.2 times (21 days).	1.5-fold ↑ in vitro tube formation	ROS↓60%	Mn^{2+} catalyzes H_2O_2 decomposition to $H_2O + O_2$	Cell viability: 95.3±3.2% ($p<0.05$)	[129]
Vitoss BA (β-TCP+20% 45S5 BG)	ALP activity increased by 1.7 times (7 days).	N/A	IL-1β↓25%	BG ionic microenvironment promotes RUNX2 nuclear translocation	Mechanical strength recovery rate ↑30% ($p<0.01$)	[96]

Notes: 1. Symbols & Statistical Conventions:↑: Increase (eg, "CD31↑1.8-fold" = 1.8× higher CD31 expression); ↓: Decrease (eg, "TNF-α↓30%" = 30% TNF-α reduction); p-values: $p<0.05$, $p<0.01$, $p<0.001$ (two-tailed *t*-test). 2. Assays & Metrics: μCT: Micro-computed tomography quantification; MT staining: Masson's trichrome staining for vascular density assessment; ROS scavenging: Measured via DCFH-DA probe assay. 3. Mechanistic Insights: M1/M2 polarization: Macrophage phenotype switching (pro-inflammatory/anti-inflammatory); Wnt/β-catenin pathway: Regulates mesenchymal stem cell osteogenic differentiation; PI3K/AKT pathway: Mediates cell survival/proliferation signaling. 4. Material Properties: PDA coating: Polydopamine modification enables sustained BMP-2 release (85% over 28 days); NIR responsiveness: Ti3C2 MXene mediates photothermal synergy (808nm laser).

Table 3 Comparative Analysis of β-TCP Composite Scaffold Fabrication Techniques

Fabrication Technique	Precision Control	Cost	Customization Capability	Scalability	Typical Applications	Limitations	References
3D Gel Printing with Sintering	Porosity 50%-90%, uniform and controllable pore size	High	High (complex geometries)	Moderate (equipment-dependent)	Trabecular bone tissue engineering	Material brittleness, high sintering temperature	[76]
FDM 3D Printing	Adjustable pore shape with limited resolution (~400μm layer thickness)	Low	High (CAD design)	High (industrial scale)	Large-scale bone defect repair	Low mechanical properties, insufficient pore connectivity	[73]
3D Printing +[1]/Physical Crosslinking	High microsphere loading precision (500–1500nm)	Medium	Medium	Moderate (complex process)	Infected bone defect treatment (antibacterial/osteogenic)	Challenges in matching drug release rate with degradation	[130]
Electrospinning Technology	Nanoscale fiber diameter (3–5000 nm), ECM-mimetic structures	High	Low (morphological constraints)	Low (small batch)	Maxillofacial bone regeneration (bionic structures)	Insufficient mechanical strength, rapid degradation	[102]
DIW with Template Sacrifice Method (SiO2/CNT)	Dual-scale pore control: macropores (~400μm) and micropores (fibrous/spherical)	Medium	High (hierarchical design)	High (template replaceable)	Vascularized bone regeneration	Multi-step process, time-consuming	[119]
Supercritical CO2 Foaming	Uniform porosity (65–67%) and pore size	Medium	Low (morphology constraints)	High (mass production)	Intraoperatively moldable elastic bone substitutes	Poor long-term degradation stability	[122]
Solvent Casting & Compression Molding	Single pore structure (mold-dependent)	Low	Low	Moderate (mold limitations)	Load-bearing bone defect repair	Poor pore connectivity, mismatch between degradation and regeneration rates	[16]
Low-temperature Deposition Manufacturing (LDM)	High precision (±50μm), controlled porosity (400μm) and layer thickness	High	High (parameter tunable)	Moderate (specialized equipment)	Cranial regeneration (clinical translation potential)	High equipment cost, complex material formulations	[75]
Co-precipitation (Fe/Sr doping)	Uniform ion doping (0.2–1.0 mol%)	Low	Low (chemical control)	High (composition flexibility)	Bone grafting/cancer thermotherapy (magnetic functionalization)	Weak mechanical properties, unpredictable degradation rates	[85]
DLP Photopolymerization 3D Printing	Dual-scale pore regulation: macro/micro (±20μm precision)	High	High (CAD design)	Moderate (viscosity constraints)	Patient-specific bone repair (high-precision scaffolds)	Expensive equipment, potential biocompatibility issues from resin residues	[71]

Notes: 1. Key Parameter Definitions: Customization scalability: Ability to tailor scaffold geometry while maintaining structural/functional fidelity; Dual-scale porosity: Simultaneous control of macropores (>300μm) and micropores (<50μm) via template sacrifice. 2. Technical Limitations: Material stability: Includes brittleness (3D gel-printed scaffolds) and rapid degradation (electrospun fibers); Biocompatibility concerns: Residual resin toxicity in DLP photopolymerization. Pore connectivity: FDM-printed scaffolds show <60% interlayer connectivity (μCT analysis). 3. Symbol Conventions: ~: Approximate values (eg, ~400μm layer thickness); ±: Precision tolerance (eg, ±50μm). 4. Application Trade-offs: Mechanical strength hierarchy: Solvent casting (92MPa) > DIW (30–60MPa) > supercritical foaming (2.89MPa); Degradation matching: Co-precipitation shows 35% variability in degradation rates (in vitro vs in vivo).

significantly affect their practical applicability in complex bone repair scenarios. For instance, while 3D gel printing enables precise regulation of porosity (up to 90%) to mimic cancellous bone structure, its high sintering temperatures may increase material brittleness.[76] Conversely, techniques combining electrospinning with physical cross-linking allow drug loading via nanoscale fibers (500–1500 nm) but encounter challenges in synchronizing degradation rates with antimicrobial agent release.[130] This comparative analysis highlights the trade-offs between multiscale structural control, bioactivity preservation, and clinical translation feasibility across manufacturing strategies, offering essential guidance for selecting fabrication processes that meet specific β-TCP composite requirements in bone regeneration applications.

Clinical Translation in Bone Repair

While preclinical studies have demonstrated the osteogenic potential of β-TCP composites, their clinical translation requires rigorous evaluation through well-designed trials. Current clinical evidence comprises both randomized controlled trials (RCTs) and observational studies, with varying levels of evidence strength.

β-TCP is widely used in orthopedics, particularly in dentistry, due to its inorganic composition, which closely resembles that of the inorganic layer of cortical bone. In dentistry, β-TCP is currently utilized for alveolar bone preservation and alveolar bone augmentation. Cao et al evaluated the effectiveness of β-TCP in enhancing the regeneration of bone defects and periodontal conditions, specifically in the second molar area after mandibular third molar extraction, through a randomized controlled study.[133] The study (RCT, n=15) found that β-TCP promoted more vertical bone regeneration and significantly reduced the probing depth compared to natural healing. Han et al used recombinant human bone morphogenetic protein-2 (rhBMP-2) with β-TCP as a bone-grafting material, achieving excellent alveolar bone preservation in patients with extracted teeth (RCT, n=84).[134] Wei et al applied E. coli-derived recombinant human bone morphogenetic protein-2 (EhBMP-2) combined with bionic calcium phosphate-coated functionalized β-TCP (EhBMP-2/BioCaP/β-TCP) in patients requiring dental implants post single-root extractions.[135] This study (RCT, n=45) compared the EhBMP-2/BioCaP/β-TCPem-treated group with a natural healing group and a control group treated with β-TCP alone. Biopsy samples obtained six weeks after tooth extraction were used to assess new bone formation, residual materials, and unmineralized tissues. Patients in the EhBMP-2/BioCaP/β-TCP group exhibited significantly higher bone formation and new bone volume density in both the marginal and central regions of the alveolar fossa. In contrast, the natural healing group showed bone trabeculae primarily around the alveolus, while the central region was dominated by fibrous tissue. The group treated with β-TCP alone demonstrated the least new bone formation. Notably, the incidence of adverse events and soft tissue healing scores were comparable across all groups. These results highlight the efficacy of EhBMP-2/BioCaP/β-TCP as a biocompatible material that promotes bone growth. β-TCP has also been used to repair mandibular defects. In contrast, Schönegg et al reported a case study of a 63-year-old female patient with significant horizontal bone loss in the posterior aspect of the mandible using a customized β-TCP stent.[136] After a two-year follow-up, the patient's oral cavity and peri-implant environment remained in good health.

The benefits of platelet-rich fibrin (PRF) in cell proliferation, migration, adhesion, differentiation, and inflammatory modulation have been well documented, as reported by Strauss et al in their systematic review.[137] Baghele et al conducted an RCT (n=42) comparing β-TCP, with a composite of β-TCP and PRF for treating bone defects.[138] The β-TCP and PRF group demonstrated significant improvements in probing depth and clinical attachment levels after six months.

Similarly, platelet-rich plasma (PRP), a source of growth factors, has been widely recognized for promoting tissue repair and regeneration.[139] Kavitha indicated through a case report that chronic periapical lesions treated with PRP/β-TCP and PRF/β-TCP resulted in significant increases in bone mineral density at six and twelve months post-operation.[140] Both combinations effectively promoted bone regeneration and accelerated healing.

In treating avascular necrosis of the femoral head (ANFH), Lu et al developed a β-TCP system to promote vascular regeneration and bone tissue repair, combining porous β-TCP rods and dense β-TCP particles.[20] This system was evaluated in 246 hips from 214 patients (a multi-center prospective open-label clinical trial). The β-TCP rods directed the blood flow from the greater trochanter and neck of the femur to the necrotic area, healing the ANFH (Figure 9A and B). The β-TCP particles prevented post-operative femoral head collapse (Figure 9B). Figure 9A and C demonstrate the compaction of the β-TCP pellet into the femoral head and the subsequent insertion of the Clinical outcomes for

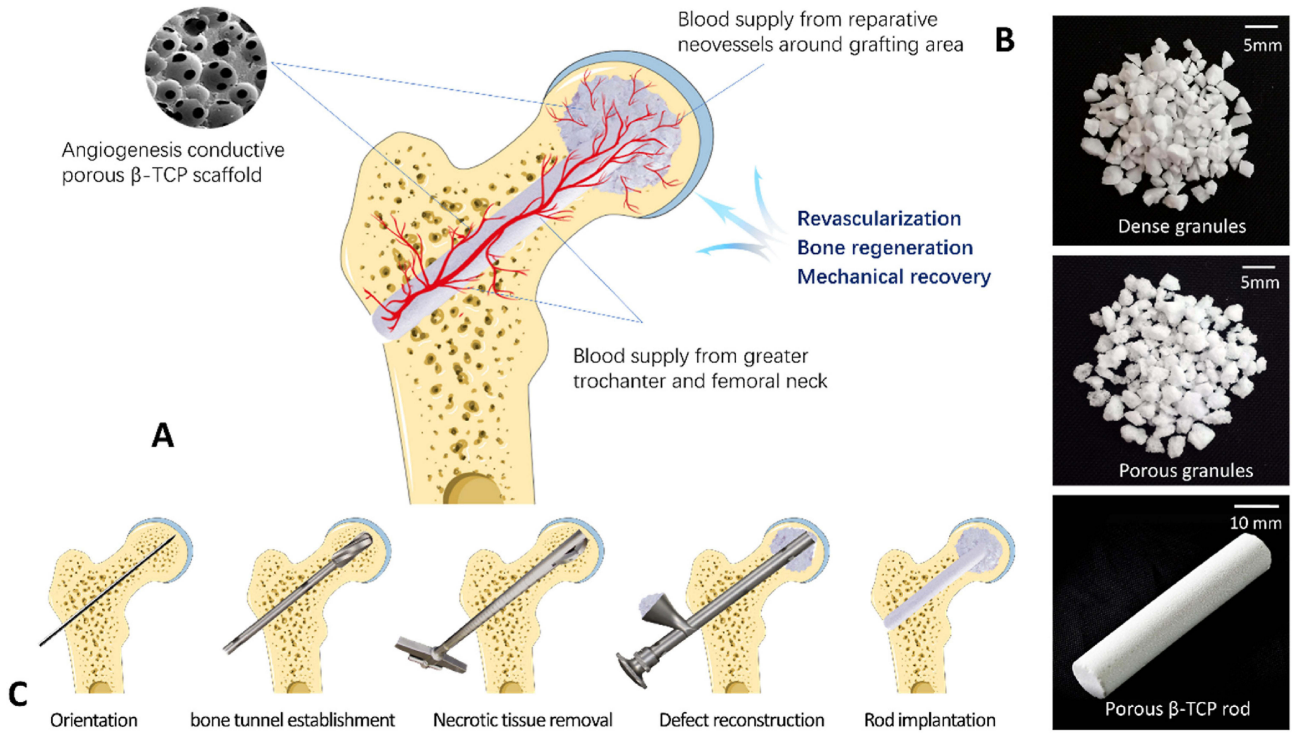

Figure 9 Schematic of the surgical design of the β-TCP system for ANFH treatment. (**A**) Blood vessels from the proximal femur and reparative neovessels around the grafting area were directed into the femoral head through the implanted porous β-TCP scaffold, thus facilitating revascularization, bone regeneration and mechanical recovery; (**B**) The β-TCP system used for ANFH, including dense granules, porous granules, and a porous rod. (**C**) The main surgical procedure, included orientation, bone tunnel establishment, necrotic tissue removal, defect reconstruction, and rod implantation. Reproduced from Lu Y, Chen X, Lu X, et al. Reconstructing avascular necrotic femoral head through a bioactive β-TCP system: from design to application. Bioact Mater. 2023;28:495–510. © 2023 The Authors. Publishing services by Elsevier B.V. on behalf of KeAi Communications Co. Ltd.CC-BY.[20]

association research circulation osseous (ARCO) stage II lesions were significantly better than those for stage III relative to pre-operative status at the post-operative follow-up. Hip function imaging findings and pain scores showed significant enhancements. More importantly, implantation of the β-TCP stent rapidly achieved adequate vascularization, effectively introducing an abundant blood supply to the necrotic area at the implantation site. This study confirmed the significant potential of the β-TCP system in treating ANFH, especially in younger populations with early-stage disease.

β-TCP rod into the femoral head. For shoulder instability, Shen explored the effectiveness of composite anchors made from biocomposites consisting of 85% PLA and 15% β-TCP in 74 cases of rostral metastasis surgery (a single-center retrospective case series).[141] The mean CT values (HU values) in the anchor implantation region were significantly higher than those in the articular fossa dome during the two-year post-operative follow-up evaluation, suggesting that the biocomposite has excellent osseointegration capabilities.

In the treatment of tibial fractures, β-TCP has also been used clinically. Seebach et al applied a β-TCP stent for open reduction internal fixation (ORIF) in 94 patients with proximal humerus fractures (RCT, n=94), with bones healing well after 12 weeks of treatment.[142] This further confirms the positive effects of β-TCP in promoting bone defect repair. Chu et al, on the other hand, evaluated the efficacy of using SECCS-prepared BMSC/β-TCP compared to β-TCP alone for treating depressed tibial plateau fractures using imaging and Lysholm score, in a retrospective non-randomized controlled trial.[143] MSC/β-TCP composites prepared using SECCS technology can effectively repair bone defects, promoting bone tissue regeneration, and accelerating the recovery of joint function.

While RCTs provide robust evidence, several studies—such as Schönegg et al's case report (n=1), Kavitha et al's case series, and Shen et al's retrospective analysis—rely on non-RCT designs. These lack randomization, adequate controls, or sufficient sample sizes, introducing potential bias and limiting generalizability. For example, small observational studies (eg, single-center case series) may overestimate efficacy due to selection bias or short follow-up. Further large-scale, multicenter RCTs are needed to validate long-term outcomes and optimize β-TCP applications.

Conclusion

β-TCP-based composite scaffolds have emerged as a promising solution for bone defect repair, offering tunable biodegradation, enhanced osteoinductivity, and improved mechanical compatibility with host tissues. As summarized in Table 3, advances in fabrication techniques—from 3D gel printing to supercritical CO_2 foaming—have enabled precise control over scaffold architecture and functional customization. Table 1 reveals that scaffolds with 60% porosity and 22 MPa compressive strength (BMP-2-loaded β-TCP) achieve optimal bone regeneration through 24-week synchronized resorption, while rapid-degrading PLGA/β-TCP/Mg composites (63% porosity; 8-week bone bridging) prioritize rabbit calvaria bone bridging. Additionally, functional enhancements—such as magnetic responsiveness in Fe/Sr-doped scaffolds and pH-dependent degradation in PLA/β-TCP systems—further tailor these constructs to mimic bone mechanics and biological cues. These innovations address critical needs in bone regeneration, particularly for complex defects requiring hierarchical vascularization and load-bearing capabilities.

However, current limitations arise from conflicting priorities in scaffold design. 3D-printed scaffolds (FDM/DLP) face mechanical fragility (<10 MPa strength) and rapid mass loss (80% in 8 weeks for nanofibers), limiting weight-bearing applications. Similarly, high-throughput methods (solvent casting) show poor pore connectivity (<30%), while precision techniques (LDM/co-precipitation) require costly setups and prolonged processing. Most critically, the mismatch between scaffold degradation rates and osteogenesis timelines risks incomplete bone regeneration or fibrous tissue encapsulation. These challenges highlight the need for material systems that balance fabrication feasibility, biomechanical performance, and dynamic bioresorption. To overcome these barriers, future research should focus on these transformative strategies:

1. Hybrid material innovation combining phase-synchronized degradation and bioactivity. Such as developing hybrid systems combining fast-degrading polymers (eg, PGA) and slow-resorbing β-TCP with Mg/Sr doping to align degradation phases with bone repair. And enhancing osteoinduction via bioactive surface engineering (eg, MXene coatings, BMP-2-loaded alginate microbeads) while preserving bulk mechanical stability.
2. Intelligent fabrication platforms integrating dynamic responsiveness and AI-driven design. For example, advancing 4D-printed dynamic scaffolds (eg, NIR-responsive PLA/β-TCP composites) to enable pore expansion during vascular invasion. Moreover, optimizing architectures using machine learning to obtain appropriate pore geometries and dopant ratios may be a promising strategy.
3. Translational validation frameworks bridging preclinical and clinical gaps. For instance, establishing standardized metrics linking micro-CT bone volume to real-time Ca^{2+}/PO_4^{3-} release via biodegradable sensors. Furthermore, scaling clinical-grade manufacturing (eg, LDM) through industry partnerships to address the cost barrier.

Through the above strategies, β-TCP composites are poised to redefine personalized bone repair, offering tailored therapies for complex defects unaddressed by conventional implants.

Abbreviations

β-TCP, β-tricalcium phosphate; BMSCs, bone marrow mesenchymal stem cells; RANKL, Osteoblasts secrete the osteoclast differentiation factor; HCL, hydrochloric acid; OPG, osteoprotegerin; VEGF, vascular endothelial cells; TGF-α, transforming growth factor-alpha interleukin 6 IL-6; CCL2, chemokine-coordinated ligand 2; IL-10, interleukin-10; TGF-β, transforming growth factor-β; ROS, reactive oxygen species; BMP-2, bone morphogenetic protein-2; HA, hydroxyapatite; FDM, Fused Deposition Molding; PCL, Polycaprolactone; PGA, polyglycolic acid; ADA, alginate dialdehyde; PDL-02, PDL-02a, and PDL-04, polylysine polymers; PLA, polylactic acid; PLGA, polylactic acid-hydroxyacetic acid copolymerization; LTDM, low-temperature deposition manufacturing; TiO_2, titanium dioxide; POFC, poly (1,8-octanediol-co-F127 citrate); PLGA, lactic acid-glycolic acid copolymer; ah-BM-MSCs, adult bone marrow mesenchymal stem cells; ALP, alkaline phosphatase; CaSO4, calcium sulfate; GelMA, gelatinized methacrylic acid; PDA, Polydopamine; AM, alginate microbeads; ARS, alizarin red S-staining; RT-qPCR, quantitative real-time polymerase chain reaction; TGF-β1, transforming growth factor-β1; MgO, magnesium oxide; ZnO, zinc oxide; SrO,

strontium oxide; SiO2, silicon dioxide; MXene, *Ti3C2Tx*; ICT, Icariin; NIR, near-infrared; BG, bioglass; PLLA, poly (lactic acid); PTMC, poly (trimethylene carbonate); DBM, demineralized bone matrix; MoS2, molybdenum disulfide; IGF-1, growth factor-1; SF, sericin; MTT, methyl thiazolyl tetrazolium colorimetry; SEM, scanning electron microscopy; HE, hematoxylin-eosin; HUVECs, human umbilical vein endothelial cells; SECCS, screen-rich-combine circulating system; PDLLA, poly-D/L-lactic acid; DIW, Direct Ink Writing; PLCL, poly(lactic-co-ε-caprolactone); EPCs, endothelial progenitor cells; LT-RP, low-temperature rapid prototyping; CuB, cucurbitacin B; VEGFR-2, vascular endothelial growth factor receptor 2; PLGA, poly (lactic acid)-poly (glycolic acid); MET, metformin; CTS, chitosan; SBA-15, mesoporous silica; P(3HO), poly (3-hydroxyoctanoic acid); UPPE, unsaturated polyphosphate ester; TTC, tetracycline; rhBMP-2, recombinant human bone morphogenetic protein-2; EhBMP-2, human bone morphogenetic protein-2; PRF, platelet-rich fibrin; PRP, platelet-rich plasma; ANFH, avascular necrosis of the femoral head; ARCO, association research circulation osseous; ORIF, open reduction internal fixation; PMNs, neutrophils; IFN-γ, Interferon – gamma; AAMs, alternative activation of macrophages; IL-4, interleukin-4; IL-13, interleukin-13ARG1 arginase 1; INOS, inducible nitric oxide synthase; Histone H3 lysine 18, histone h3 Lysine 18 lactylation; PDGF-BB, platelet-derived growth factor-bb; EC-to-OSB, endothelial-to-osteoblast conversion; TLR, toll-like receptor; Osx, Osterix; OPN, osteopontin; OCN, osteocalcin; ENPP1, ectonucleotide pyrophosphatase/phosphodiesterase 1; HTRA1, high temperature requirement A1; CCN2, connective tissue growth factor; IL1RN, interleukin-1 receptor antagonist; EIF2AK2, eukaryotic translation initiation factor 2-alpha kinase 2; NRL, natural rubber latex membrane; CaSR, calcium-sensing receptor.

Consent for Publication

All authors agree to publication.

Funding

This study was supported by the Funding for Scientific Research Projects from Wuhan Municipal Health Commission (grant numbers: WX23J01, WX23A17).

Disclosure

The author(s) report no conflicts of interest in this work.

References

1. World Health Organization [homepage on the Internet]. Ageing and health. 2021. Available from: https://www.who.int/zh/news-room/fact-sheets/detail/ageing-and-health. Accessed April 18, 2025.
2. Hoogendijk EO, Afilalo J, Ensrud KE, Kowal P, Onder G, Fried LP. Frailty: implications for clinical practice and public health. *Lancet*. 2019;394(10206):1365–1375. doi:10.1016/S0140-6736(19)31786-6
3. Campana V, Milano G, Pagano E, et al. Bone substitutes in orthopaedic surgery: from basic science to clinical practice. *J Mater Sci Mater Med*. 2014;25(10):2445–2461. doi:10.1007/s10856-014-5240-2
4. Liang B, Burley G, Lin S, Shi YC. Osteoporosis pathogenesis and treatment: existing and emerging avenues. *Cell Mol Biol Lett*. 2022;27(1):72. doi:10.1186/s11658-022-00371-3
5. Vos T, Abajobir AA, Abate KH, et al. Global, regional, and national incidence, prevalence, and years lived with disability for 328 diseases and injuries for 195 countries, 1990–2016: a systematic analysis for the Global Burden of Disease Study 2016. *Lancet*. 2017;390 (10100):1211–1259. doi:10.1016/S0140-6736(17)32154-2
6. Quek J, Vizetto-Duarte C, Teoh SH, Choo Y. Towards stem cell therapy for critical-sized segmental bone defects: current trends and challenges on the path to clinical translation. *J Funct Biomater*. 2024;15(6):145. doi:10.3390/jfb15060145
7. Van Der Stok J, Van Lieshout EMM, El-Massoudi Y, Van Kralingen GH, Patka P. Bone substitutes in the Netherlands—a systematic literature review. *Acta Biomater*. 2011;7(2):739–750. doi:10.1016/j.actbio.2010.07.035
8. Annamalai RT, Hong X, Schott NG, Tiruchinapally G, Levi B, Stegemann JP. Injectable osteogenic microtissues containing mesenchymal stromal cells conformally fill and repair critical-size defects. *Biomaterials*. 2019;208:32–44. doi:10.1016/j.biomaterials.2019.04.001
9. Zhang X, Li Y, Chen YE, Chen J, Ma PX. Cell-free 3D scaffold with two-stage delivery of miRNA-26a to regenerate critical-sized bone defects. *Nat Commun*. 2016;7:10376. doi:10.1038/ncomms10376
10. Schemitsch EH. Size matters: defining critical in bone defect size! *J Orthop Trauma*. 2017;31(Suppl 5):S20–S22. doi:10.1097/BOT.0000000000000978
11. Schmidt AH. Autologous bone graft: is it still the gold standard? *Injury*. 2021;52:S18–S22. doi:10.1016/j.injury.2021.01.043
12. Fernandes GVO, Castro F, Pereira RM, et al. Critical-size defects reconstruction with four different bone grafts associated with e-PTFE membrane: a histomorphometric experimental in vivo study. *Clin Oral Implants Res*. 2024;35(2):167–178. doi:10.1111/clr.14210

13. Fernandez de Grado G, Keller L, Idoux-Gillet Y, et al. Bone substitutes: a review of their characteristics, clinical use, and perspectives for large bone defects management. *J Tissue Eng*. 2018;9:2041731418776819. doi:10.1177/2041731418776819
14. Motta SHG, Soares APR, Fernandes JCH, Fernandes GVO. Histological assessment of bone regeneration in the maxilla with homologous bone graft: a feasible option for maxillary bone reconstruction. *J Renew Mater*. 2024;12(1):131–148. doi:10.32604/jrm.2023.043940
15. Maghsoudlou MA, Nassireslami E, Saber-Samandari S, Khandan A. Bone regeneration using bio-nanocomposite tissue reinforced with bioactive nanoparticles for femoral defect applications in medicine. *Avicenna J Med Biotechnol*. 2020;12(2):68–76.
16. Kumar A, Mir M, Aldulijan I, et al. Load-bearing biodegradable PCL-PGA-beta TCP scaffolds for bone tissue regeneration. *J Biomed Mater Res B Appl Biomater*. 2021;109(2):193–200. doi:10.1002/jbm.b.34691
17. Lee S, Kim JH, Kim YH, et al. Sustained BMP-2 delivery via alginate microbeads and polydopamine-coated 3D-Printed PCL/β-TCP scaffold enhances bone regeneration in long bone segmental defects. *J Orthop Transl*. 2024;49:11–22. doi:10.1016/j.jot.2024.08.013
18. Zhang Y, He F, Zhang Q, Lu H, Yan S, Shi X. 3D-printed flat-bone-mimetic bioceramic scaffolds for cranial restoration. *Research*. 2023;6:0255. doi:10.34133/research.0255
19. Li C, Sun F, Tian J, et al. Continuously released Zn2+ in 3D-printed PLGA/β-TCP/Zn scaffolds for bone defect repair by improving osteoinductive and anti-inflammatory properties. *Bioact Mater*. 2023;24:361–375. doi:10.1016/j.bioactmat.2022.12.015
20. Lu Y, Chen X, Lu X, et al. Reconstructing avascular necrotic femoral head through a bioactive β-TCP system: from design to application. *Bioact Mater*. 2023;28:495–510. doi:10.1016/j.bioactmat.2023.06.008
21. Gasperini FM, Fernandes GVO, Mitri FF, et al. Histomorphometric evaluation, SEM, and synchrotron analysis of the biological response of biodegradable and ceramic hydroxyapatite-based grafts: from the synthesis to the bed application. *Biomed Mater*. 2023;18(6):065023. doi:10.1088/1748-605X/ad0397
22. Feng X, Ma L, Liang H, et al. Osteointegration of 3D-printed fully porous polyetheretherketone scaffolds with different pore sizes. *ACS Omega*. 2020;5(41):26655–26666. doi:10.1021/acsomega.0c03489
23. Liu B, Lun DX. Current application of β-tricalcium phosphate composites in orthopaedics. *Orthop Surg*. 2012;4(3):139–144. doi:10.1111/j.1757-7861.2012.00189.x
24. Abdullah MR, Goharian A, Abdul Kadir MR, Wahit MU. Biomechanical and bioactivity concepts of polyetheretherketone composites for use in orthopedic implants-a review. *J Biomed Mater Res A*. 2015;103(11):3689–3702. doi:10.1002/jbm.a.35480
25. Lu H, Zhou Y, Ma Y, et al. Current application of beta-tricalcium phosphate in bone repair and its mechanism to regulate osteogenesis. *Front Mater*. 2021;8:698915. doi:10.3389/fmats.2021.698915
26. Liang W, Zhou C, Bai J, et al. Prospective applications of bioactive materials in orthopedic therapies: a review. *Heliyon*. 2024;10(16):e36152. doi:10.1016/j.heliyon.2024.e36152
27. Zhang L, Yang G, Johnson BN, Jia X. Three-dimensional (3D) printed scaffold and material selection for bone repair. *Acta Biomater*. 2019;84:16–33. doi:10.1016/j.actbio.2018.11.039
28. Gerstenfeld LC, Cullinane DM, Barnes GL, Graves DT, Einhorn TA. Fracture healing as a post-natal developmental process: molecular, spatial, and temporal aspects of its regulation. *J Cell Biochem*. 2003;88(5):873–884. doi:10.1002/jcb.10435
29. Nakashima K, Zhou X, Kunkel G, et al. The novel zinc finger-containing transcription factor osterix is required for osteoblast differentiation and bone formation. *Cell*. 2002;108(1):17–29. doi:10.1016/S0092-8674(01)00622-5
30. Mak KK, Bi Y, Wan C, et al. Hedgehog signaling in mature osteoblasts regulates bone formation and resorption by controlling PTHrP and RANKL expression. *Dev Cell*. 2008;14(5):674–688. doi:10.1016/j.devcel.2008.02.003
31. Martin I, Muraglia A, Campanile G, Cancedda R, Quarto R. Fibroblast growth factor-2 supports ex vivo expansion and maintenance of osteogenic precursors from human bone marrow*. *Endocrinology*. 1997;138(10):4456–4462. doi:10.1210/endo.138.10.5425
32. Chen Q, Shou P, Zheng C, et al. Fate decision of mesenchymal stem cells: adipocytes or osteoblasts? *Cell Death Differ*. 2016;23(7):1128–1139. doi:10.1038/cdd.2015.168
33. Jacome-Galarza CE, Lee SK, Lorenzo JA, Aguila HL. Identification, characterization, and isolation of a common progenitor for osteoclasts, macrophages, and dendritic cells from murine bone marrow and periphery. *J Bone Miner Res*. 2013;28(5):1203–1213. doi:10.1002/jbmr.1822
34. Boyle WJ, Simonet WS, Lacey DL. Osteoclast differentiation and activation. *Nature*. 2003;423(6937):337–342. doi:10.1038/nature01658
35. Teitelbaum SL. Bone resorption by osteoclasts. *Science*. 2000;289(5484):1504–1508. doi:10.1126/science.289.5484.1504
36. Long F. Building strong bones: molecular regulation of the osteoblast lineage. *Nat Rev Mol Cell Biol*. 2011;13(1):27–38. doi:10.1038/nrm3254
37. Compton JT, Lee FY. A review of osteocyte function and the emerging importance of sclerostin. *J Bone Joint Surg Am*. 2014;96(19):1659–1668. doi:10.2106/JBJS.M.01096
38. Zhu S, Chen W, Masson A, Li YP. Cell signaling and transcriptional regulation of osteoblast lineage commitment, differentiation, bone formation, and homeostasis. *Cell Discov*. 2024;10(1):71. doi:10.1038/s41421-024-00689-6
39. Glass DA, Karsenty G. Canonical wnt signaling in osteoblasts is required for osteoclast differentiation. *Ann N Y Acad Sci*. 2006;1068(1):117–130. doi:10.1196/annals.1346.015
40. Robling AG, Niziolek PJ, Baldridge LA, et al. Mechanical stimulation of bone in vivo reduces osteocyte expression of Sost/sclerostin. *J Biol Chem*. 2008;283(9):5866–5875. doi:10.1074/jbc.M705092200
41. Salhotra A, Shah HN, Levi B, Longaker MT. Mechanisms of bone development and repair. *Nat Rev Mol Cell Biol*. 2020;21(11):696–711. doi:10.1038/s41580-020-00279-w
42. Orvalho JM, Fernandes JCH, Moraes Castilho R, Fernandes GVO. The macrophage's role on bone remodeling and osteogenesis: a systematic review. *Clin Rev Bone Miner Metab*. 2023;21(1):1–13. doi:10.1007/s12018-023-09286-9
43. Claes L, Recknagel S, Ignatius A. Fracture healing under healthy and inflammatory conditions. *Nat Rev Rheumatol*. 2012;8(3):133–143. doi:10.1038/nrrheum.2012.1
44. Gordon S, Fo M. Alternative activation of macrophages: mechanism and functions. *Immunity*. 2010;32(5):593–604. doi:10.1016/j.immuni.2010.05.007
45. Chen Z, Mao X, Tan L, et al. Osteoimmunomodulatory properties of magnesium scaffolds coated with β-tricalcium phosphate. *Biomaterials*. 2014;35(30):8553–8565. doi:10.1016/j.biomaterials.2014.06.038
46. Sica A, Mantovani A. Macrophage plasticity and polarization: in vivo veritas. *J Clin Invest*. 2012;122(3):787–795. doi:10.1172/JCI59643

47. Yu R, Han H, Chu S, et al. Cullin 4B-RING E3 ligase negatively regulates the immunosuppressive capacity of mesenchymal stem cells by suppressing iNOS. *Cell Death Differ*. 2025;32(1):149–161. doi:10.1038/s41418-024-01359-6
48. Linton MF, Moslehi JJ, Babaev VR. Akt Signaling in Macrophage Polarization, Survival, and Atherosclerosis. *Int J Mol Sci*. 2019;20(11):2703. doi:10.3390/ijms20112703
49. Zhang Y, Jiang H, Dong M, et al. Macrophage MCT4 inhibition activates reparative genes and protects from atherosclerosis by histone H3 lysine 18 lactylation. *Cell Rep*. 2024;43(5):114180. doi:10.1016/j.celrep.2024.114180
50. Xia L, Wang X, Liu L, et al. lnc-BAZ2B promotes M2 macrophage activation and inflammation in children with asthma through stabilizing BAZ2B pre-mRNA. *J Allergy Clin Immunol*. 2021;147(3):921–932.e9. doi:10.1016/j.jaci.2020.06.034
51. Ghafouri-Fard S, Abak A, Tavakkoli Avval S, Shoorei H, Taheri M, Samadian M. The impact of non-coding RNAs on macrophage polarization. *Biomed Pharmacother*. 2021;142:112112. doi:10.1016/j.biopha.2021.112112
52. Qiang H, Hou C, Zhang Y, et al. CaP-coated Zn-Mn-Li alloys regulate osseointegration via influencing macrophage polarization in the osteogenic environment. *Regen Biomater*. 2023;10:rbad051. doi:10.1093/rb/rbad051
53. Rafieerad A, Yan W, Sequiera GL, et al. Application of Ti3 C2 MXene quantum dots for immunomodulation and regenerative medicine. *Adv Healthc Mater*. 2019;8(16):e1900569. doi:10.1002/adhm.201900569
54. Schröder K. NADPH oxidases in bone homeostasis and osteoporosis. *Free Radic Biol Med*. 2019;132:67–72. doi:10.1016/j.freeradbiomed.2018.08.036
55. Phull AR, Nasir B, Haq IU, Kim SJ. Oxidative stress, consequences and ROS mediated cellular signaling in rheumatoid arthritis. *Chem Biol Interact*. 2018;281:121–136. doi:10.1016/j.cbi.2017.12.024
56. Jia WT, Fu Q, Huang WH, Zhang CQ, Rahaman MN. Comparison of borate bioactive glass and calcium sulfate as implants for the local delivery of teicoplanin in the treatment of methicillin-resistant staphylococcus aureus-induced osteomyelitis in a rabbit model. *Antimicrob Agents Chemother*. 2015;59(12):7571–7580. doi:10.1128/AAC.00196-15
57. ElHawary H, Baradaran A, Abi-Rafeh J, Vorstenbosch J, Xu L, Efanov JI. Bone healing and inflammation: principles of fracture and repair. *Semin Plast Surg*. 2021;35(3):198–203. doi:10.1055/s-0041-1732334
58. Hankenson KD, Dishowitz M, Gray C, Schenker M. Angiogenesis in bone regeneration. *Injury*. 2011;42(6):556–561. doi:10.1016/j.injury.2011.03.035
59. Bessa PC, Casal M, Reis RL. Bone morphogenetic proteins in tissue engineering: the road from laboratory to clinic, part II (BMP delivery). *J Tissue Eng Regen Med*. 2008;2(2–3):81–96. doi:10.1002/term.74
60. Wang J, Gao Y, Cheng P, et al. CD31hiEmcnhi vessels support new trabecular bone formation at the frontier growth area in the bone defect repair process. *Sci Rep*. 2017;7(1):4990. doi:10.1038/s41598-017-04150-5
61. Ma G, Han Y, Tang W, et al. Endothelial-to-osteoblast conversion maintains bone homeostasis through Kindlin-2/Piezo1/TGFβ/Runx2 axis. *Protein Cell*. 2024;16:pwae066. doi:10.1093/procel/pwae066
62. Bohner M, Santoni BLG, Döbelin N. β-tricalcium phosphate for bone substitution: synthesis and properties. *Acta Biomater*. 2020;113:23–41. doi:10.1016/j.actbio.2020.06.022
63. Winkler T, Sass FA, Duda GN, Schmidt-Bleek K. A review of biomaterials in bone defect healing, remaining shortcomings and future opportunities for bone tissue engineering: the unsolved challenge. *Bone Jt Res*. 2018;7(3):232–243. doi:10.1302/2046-3758.73.BJR-2017-0270.R1
64. Yamada S, Heymann D, Bouler JM, Daculsi G. Osteoclastic resorption of calcium phosphate ceramics with different hydroxyapatite/beta-tricalcium phosphate ratios. *Biomaterials*. 1997;18(15):1037–1041. doi:10.1016/s0142-9612(97)00036-7
65. Chai YC, Carlier A, Bolander J, et al. Current views on calcium phosphate osteogenicity and the translation into effective bone regeneration strategies. *Acta Biomater*. 2012;8(11):3876–3887. doi:10.1016/j.actbio.2012.07.002
66. Yuan H, Fernandes H, Habibovic P, et al. Osteoinductive ceramics as a synthetic alternative to autologous bone grafting. *Proc Natl Acad Sci U S A*. 2010;107(31):13614–13619. doi:10.1073/pnas.1003600107
67. Lee W, Prat D, Chao W, Farber DC, Wang C, Wapner KL. The efficiency of highly porous β-tricalcium phosphate with bone marrow aspirate concentrate in midfoot joint arthrodesis. *Foot Ankle Spec*. 2023;19386400231213177. doi:10.1177/19386400231213177
68. Ducheyne P, Qiu Q. Bioactive ceramics: the effect of surface reactivity on bone formation and bone cell function. *Biomaterials*. 1999;20(23–24):2287–2303. doi:10.1016/s0142-9612(99)00181-7
69. Hench LL, Jones JR. Bioactive glasses: frontiers and challenges. *Front Bioeng Biotechnol*. 2015;3:194. doi:10.3389/fbioe.2015.00194
70. Kneser U, Schaefer DJ, Polykandriotis E, Horch RE. Tissue engineering of bone: the reconstructive surgeon's point of view. *J Cell Mol Med*. 2006;10(1):7–19. doi:10.1111/j.1582-4934.2006.tb00287.x
71. Xu S, Zhang H, Li X, et al. Fabrication and biological evaluation of porous β-TCP bioceramics produced using digital light processing. *Proc Inst Mech Eng H*. 2022;236(2):286–294. doi:10.1177/09544119211041186
72. Umrath F, Schmitt LF, Kliesch SM, et al. Mechanical and functional improvement of β-TCP scaffolds for use in bone tissue engineering. *J Funct Biomater*. 2023;14(8):427. doi:10.3390/jfb14080427
73. Wang W, Liu P, Zhang B, et al. Fused deposition modeling printed PLA/Nano β-TCP composite bone tissue engineering scaffolds for promoting osteogenic induction function. *Int J Nanomed*. 2023;18:5815–5830. doi:10.2147/IJN.S416098
74. Wang B, Ye X, Chen G, et al. Fabrication and properties of PLA/β-TCP scaffolds using liquid crystal display (LCD) photocuring 3D printing for bone tissue engineering. *Front Bioeng Biotechnol*. 2024;12:1273541. doi:10.3389/fbioe.2024.1273541
75. Zhou Y, Hu J, Li B, Xia J, Zhang T, Xiong Z. Towards the clinical translation of 3D PLGA/β-TCP/Mg composite scaffold for cranial bone regeneration. *Materials*. 2024;17(2):352. doi:10.3390/ma17020352
76. Xulin H, Hu L, Liang Q, et al. 369Fabrication of 3D gel-printed β-tricalcium phosphate/titanium dioxide porous scaffolds for cancellous bone tissue engineering. *Int J Bioprinting*. 2023;9(2):673. doi:10.18063/ijb.v9i2.673
77. Ge C, Chen F, Mao L, Liang Q, Su Y, Liu C. Strontium ranelate-loaded POFC/β-TCP porous scaffolds for osteoporotic bone repair. *RSC Adv*. 2020;10(15):9016–9025. doi:10.1039/c9ra08909h
78. Bohner M, Baumgart F. Theoretical model to determine the effects of geometrical factors on the resorption of calcium phosphate bone substitutes. *Biomaterials*. 2004;25(17):3569–3582. doi:10.1016/j.biomaterials.2003.10.032

79. Yuan H, Yang Z, Li Y, Zhang X, De Bruijn JD, De Groot K. Osteoinduction by calcium phosphate biomaterials. *J Mater Sci Mater Med*. 1998;9(12):723–726. doi:10.1023/a:1008950902047
80. Yassuda-Mattos DH, de Freitas Costa NM, Tavares DS, et al. Study of bone repair in rat dental socket after implantation of porous granules of Beta-Tricalcium Phosphate (β-TCP) and Magnesium-Substituted Beta-Tricalcium Phosphate (β-TCMP). *Key Eng Mater*. 2012;493–494:263–-268. doi:10.4028/www.scientific.net/KEM.493-494.263
81. Putri TS, Hayashi K, Ishikawa K. Bone regeneration using β-tricalcium phosphate (β-TCP) block with interconnected pores made by setting reaction of β-TCP granules. *J Biomed Mater Res A*. 2020;108(3):625–632. doi:10.1002/jbm.a.36842
82. Seidenstuecker M, Schmeichel T, Ritschl L, et al. Mechanical properties of the composite material consisting of β-TCP and alginate-di-aldehyde -gelatin hydrogel and its degradation behavior. *Materials*. 2021;14(5):1303. doi:10.3390/ma14051303
83. Wu H, Wei X, Liu Y, et al. Dynamic degradation patterns of porous polycaprolactone/β-tricalcium phosphate composites orchestrate macrophage responses and immunoregulatory bone regeneration. *Bioact Mater*. 2023;21:595–611. doi:10.1016/j.bioactmat.2022.07.032
84. Zhu X, Liu W, Sun Z, Yan S, Liu H, Wang Z. In Vitro Degradation Behavior of Absorbable Interface Screws. *Zhongguo Yi Liao Qi Xie Za Zhi*. 2023;47(6):598–601. doi:10.3969/j.issn.1671-7104.2023.06.002
85. Kim SM, Yoo KH, Kim H, Kim YI, Yoon SY. Simultaneous substitution of Fe and Sr in beta-tricalcium phosphate: synthesis, structural, magnetic, degradation, and cell adhesion properties. *Materials*. 2022;15(13):4702. doi:10.3390/ma15134702
86. Kakuta A, Tanaka T, Chazono M, et al. Effects of micro-porosity and local BMP-2 administration on bioresorption of β-TCP and new bone formation. *Biomater Res*. 2019;23(1):12. doi:10.1186/s40824-019-0161-2
87. López-González I, Zamora-Ledezma C, Sanchez-Lorencio MI, Tristante Barrenechea E, Gabaldón-Hernández JA, Meseguer-Olmo L. Modifications in gene expression in the process of osteoblastic differentiation of multipotent bone marrow-derived human mesenchymal stem cells induced by a novel osteoinductive porous medical-grade 3D-Printed Poly(ε-caprolactone)/β-tricalcium Phosphate Composite. *Int J Mol Sci*. 2021;22(20):11216. doi:10.3390/ijms222011216
88. Wang Q, Ye W, Ma Z, et al. 3D printed PCL/β-TCP cross-scale scaffold with high-precision fiber for providing cell growth and forming bones in the pores. *Mater Sci Eng C Mater Biol Appl*. 2021;127:112197. doi:10.1016/j.msec.2021.112197
89. Zheng C, Zhang M. 3D-printed PCL/β-TCP/CS composite artificial bone and histocompatibility study. *J Orthop Surg*. 2023;18(1):981. doi:10.1186/s13018-023-04489-8
90. Luo D, Chen B, Chen Y. Stem cells-loaded 3D-printed scaffolds for the reconstruction of alveolar cleft. *Front Bioeng Biotechnol*. 2022;10:939199. doi:10.3389/fbioe.2022.939199
91. Bonato RS, Fernandes GVDO, Calasans-Maia MD, et al. The influence of rhBMP-7 associated with nanometric hydroxyapatite coatings titanium implant on the osseointegration: a pre-clinical study. *Polymers*. 2022;14(19):4030. doi:10.3390/polym14194030
92. Wang C, Yue H, Huang W, et al. Cryogenic 3D printing of heterogeneous scaffolds with gradient mechanical strengths and spatial delivery of osteogenic peptide/TGF-β1 for osteochondral tissue regeneration. *Biofabrication*. 2020;12(2):025030. doi:10.1088/1758-5090/ab7ab5
93. Yassuda DH, Costa NFM, Fernandes GO, Alves GG, Granjeiro JM, Soares GDA. Magnesium incorporation into β-TCP reduced its *in vivo* resorption by decreasing parathormone production. *J Biomed Mater Res A*. 2013;101A(7):1986–1993. doi:10.1002/jbm.a.34502
94. Saito K, Inagaki Y, Uchihara Y, et al. MgO-enhanced β-TCP promotes osteogenesis in both in vitro and in vivo rat models. *Sci Rep*. 2024;14(1):19725. doi:10.1038/s41598-024-70512-5
95. Gu C, Chen H, Zhao Y, et al. Ti(3)C(2)T(x)@PLGA/Icaritin microspheres-modified PLGA/β-TCP scaffolds modulate Icaritin release to enhance bone regeneration through near-infrared response. *Biomed Mater*. 2024;19(5):055038. doi:10.1088/1748-605X/ad6dc9
96. Westhauser F, Karadjian M, Essers C, et al. Osteogenic differentiation of mesenchymal stem cells is enhanced in a 45S5-supplemented β-TCP composite scaffold: an in-vitro comparison of Vitoss and Vitoss BA. *PLoS One*. 2019;14(2):e0212799. doi:10.1371/journal.pone.0212799
97. Kazemi M, Dehghan MM, Azami M. Biological evaluation of porous nanocomposite scaffolds based on strontium substituted β-TCP and bioactive glass: an in vitro and in vivo study. *Mater Sci Eng C Mater Biol Appl*. 2019;105:110071. doi:10.1016/j.msec.2019.110071
98. Duan G, Lu YF, Chen HL, et al. Smurf1-targeting microRNA-136-5p-modified bone marrow mesenchymal stem cells combined with 3D-printed β-tricalcium phosphate scaffolds strengthen osteogenic activity and alleviate bone defects. *Kaohsiung J Med Sci*. 2024;40(7):621–630. doi:10.1002/kjm2.12847
99. Zavan B, Gardin C, Guarino V, et al. Electrospun PCL-based vascular grafts: in vitro tests. *Nanomaterials*. 2021;11(3):751. doi:10.3390/nano11030751
100. Patel KH, Talovic M, Dunn AJ, et al. Aligned nanofibers of decellularized muscle extracellular matrix for volumetric muscle loss. *J Biomed Mater Res B Appl Biomater*. 2020;108(6):2528–2537. doi:10.1002/jbm.b.34584
101. Chen L, Cheng L, Wang Z, et al. Corrigendum to "Conditioned medium-electrospun fiber biomaterials for skin regeneration" [Bioact. Mater. 6 (2021) 361–374]. *Bioact Mater*. 2021;6(9):2752–2753. doi:10.1016/j.bioactmat.2021.02.001
102. Ramanathan M, Shijirbold A, Okui T, et al. In vivo evaluation of bone regenerative capacity of the novel nanobiomaterial: β-Tricalcium Phosphate Polylactic Acid-co-Glycolide (β-TCP/PLLA/PGA) for use in maxillofacial bone defects. *Nanomaterials*. 2023;14(1):91. doi:10.3390/nano14010091
103. Mahmoud AH, Han Y, Dal-Fabbro R, et al. Nanoscale β-TCP-Laden GelMA/PCL composite membrane for guided bone regeneration. *ACS Appl Mater Interfaces*. 2023;15(27):32121–32135. doi:10.1021/acsami.3c03059
104. Yu DG, He W, He C, Liu H, Yang H. Versatility of electrospun Janus wound dressings. *Nanomed*. 2025;20(3):271–278. doi:10.1080/17435889.2024.2446139
105. Huang C, Wang M, Yu S, Yu DG, Bligh SWA. Electrospun fenoprofen/polycaprolactone @ tranexamic acid/hydroxyapatite nanofibers as orthopedic hemostasis dressings. *Nanomaterials*. 2024;14(7):646. doi:10.3390/nano14070646
106. Chen S, Wu X, Ding X. One-step side-by-side electrospraying of Janus particles for durable multifunctional coatings on cotton textiles. *Colloids Surf Physicochem Eng Asp*. 2025;710:136227. doi:10.1016/j.colsurfa.2025.136227
107. Zheng SY, Liu ZW, Kang HL, Liu F, Yan GP, Li F. 3D-Printed scaffolds based on poly (Trimethylene carbonate), poly(ε-Caprolactone), and β-Tricalcium phosphate. *Int J Bioprint*. 2023;9(1):641. doi:10.18063/ijb.v9i1.641
108. Giovanetti K, Tuma RB, Sant'Ana Pegorin Brasil G, et al. β-Tricalcium phosphate incorporated natural rubber latex membranes for calvarial bone defects: physicochemical, in vitro and in vivo assessment. *Int J Biol Macromol*. 2024;282:137328. doi:10.1016/j.ijbiomac.2024.137328

109. Yuan B, Wang Z, Zhao Y, et al. In vitro and in vivo study of a novel nanoscale demineralized bone matrix coated PCL/β-TCP scaffold for bone regeneration. *Macromol Biosci*. 2021;21(3):e2000336. doi:10.1002/mabi.202000336
110. Lu L, Wang H, Yang M, Wang L, Gan K. Three-dimensional-printed MPBI@β-TCP scaffold promotes bone regeneration and impedes osteosarcoma under near-infrared laser irradiation. *FASEB J*. 2023;37(5):e22924. doi:10.1096/fj.202201991R
111. Qianjuan Z, Rong S, Shengxi L, Xuanhao L, Bin L, Fuxiang S. Assessment of artificial bone materials with different structural pore sizes obtained from 3D printed polycaprolactone/β-tricalcium phosphate (3D PCL/β-TCP). *Biomed Mater*. 2024;19(6):065004. doi:10.1088/1748-605X/ad7564
112. Li R, Cheng W, Liu H, et al. Effect of mechanical loading on bone regeneration in HA/β-TCP/SF scaffolds prepared by low-temperature 3D printing in vivo. *ACS Biomater Sci Eng*. 2023;9(8):4980–4993. doi:10.1021/acsbiomaterials.3c00437
113. Gu Y, Zhang J, Zhang X, Liang G, Xu T, Niu W. Three-dimensional printed Mg-Doped β-TCP bone tissue engineering scaffolds: effects of magnesium ion concentration on osteogenesis and angiogenesis in vitro. *Tissue Eng Regen Med*. 2019;16(4):415–429. doi:10.1007/s13770-019-00192-0
114. Zhai D, Chen L, Chen Y, Zhu Y, Xiao Y, Wu C. Lithium silicate-based bioceramics promoting chondrocyte maturation by immunomodulating M2 macrophage polarization. *Biomater Sci*. 2020;8(16):4521–4534. doi:10.1039/d0bm00450b
115. Xu N, Lu D, Qiang L, et al. 3D-printed composite bioceramic scaffolds for bone and cartilage integrated regeneration. *ACS Omega*. 2023;8(41):37918–37926. doi:10.1021/acsomega.3c03284
116. Chu W, Liu Z, Gan Y, et al. Use of a novel Screen-Enrich-Combine(-biomaterials) Circulating System to fill a 3D-printed open Ti6Al4V frame with mesenchymal stem cells/β-tricalcium phosphate to repair complex anatomical bone defects in load-bearing areas. *Ann Transl Med*. 2021;9(6):454. doi:10.21037/atm-20-6689
117. Tian Y, Ma H, Yu X, et al. Biological response of 3D-printedβ-tricalcium phosphate bioceramic scaffolds with the hollow tube structure. *Biomed Mater*. 2023;18(3):034102. doi:10.1088/1748-605X/acc374
118. Toda E, Bai Y, Sha J, et al. Feasibility of application of the newly developed nano-biomaterial, β-TCP/PDLLA, in maxillofacial reconstructive surgery: a pilot rat study. *Nanomaterials*. 2021;11(2):303. doi:10.3390/nano11020303
119. Feng J, Liu J, Wang Y, Diao J, Kuang Y, Zhao N. Beta-TCP scaffolds with rationally designed macro-micro hierarchical structure improved angio/osteo-genesis capability for bone regeneration. *J Mater Sci Mater Med*. 2023;34(7):36. doi:10.1007/s10856-023-06733-3
120. Wu Y, Chen R, Chen X, Yang Y, Qiao J, Liu Y. Development of strong and tough β-TCP/PCL composite scaffolds with interconnected porosity by digital light processing and partial infiltration. *Materials*. 2023;16(3):947. doi:10.3390/ma16030947
121. Zhou M, Yang X, Li S, et al. Bioinspired channeled, rhBMP-2-coated β-TCP scaffolds with embedded autologous vascular bundles for increased vascularization and osteogenesis of prefabricated tissue-engineered bone. *Mater Sci Eng C Mater Biol Appl*. 2021;118:111389. doi:10.1016/j.msec.2020.111389
122. Pitkänen S, Paakinaho K, Pihlman H, et al. Characterisation and in vitro and in vivo evaluation of supercritical-CO2-foamed β-TCP/PLCL composites for bone applications. *Eur Cell Mater*. 2019;38:35–50. doi:10.22203/eCM.v038a04
123. Qi D, Su J, Li S, et al. 3D printed magnesium-doped β-TCP gyroid scaffold with osteogenesis, angiogenesis, immunomodulation properties and bone regeneration capability in vivo. *Biomater Adv*. 2022;136:212759. doi:10.1016/j.bioadv.2022.212759
124. Prabakaran S, Kavibharathi R, Vinothini K, Periakaruppan R, Chandrasekaran N. Surface activation of titanium implant by tricalcium phosphate ceramic based composite coating for bone tissue regeneration. *Trans Indian Ceram Soc*. 2024;83(4):252–264. doi:10.1080/0371750X.2024.2431861
125. Cheng WX, Liu YZ, Meng XB, et al. PLGA/β-TCP composite scaffold incorporating cucurbitacin B promotes bone regeneration by inducing angiogenesis. *J Orthop Transl*. 2021;31:41–51. doi:10.1016/j.jot.2021.10.002
126. Cao Y, Xiao L, Cao Y, Nanda A, Xu C, Ye Q. 3D printed β-TCP scaffold with sphingosine 1-phosphate coating promotes osteogenesis and inhibits inflammation. *Biochem Biophys Res Commun*. 2019;512(4):889–895. doi:10.1016/j.bbrc.2019.03.132
127. Hu X, Chen J, Yang S, et al. 3D printed multifunctional biomimetic bone scaffold combined with TP-Mg nanoparticles for the infectious bone defects repair. *Small*. 2024;20(40):e2403681. doi:10.1002/smll.202403681
128. Huang B, Li S, Dai S, et al. Ti(3)C(2)T(x) MXene-Decorated 3D-printed ceramic scaffolds for enhancing osteogenesis by spatiotemporally orchestrating inflammatory and bone repair responses. *Adv Sci*. 2024;11(34):e2400229. doi:10.1002/advs.202400229
129. Qian F, Huang Z, Liu W, Liu Y, He X. Functional β-TCP/MnO(2) /PCL artificial periosteum promoting osteogenic differentiation of BMSCs by reducing locally reactive oxygen species level. *J Biomed Mater Res A*. 2023;111(11):1678–1691. doi:10.1002/jbm.a.37576
130. Qiu X, Li S, Li X, et al. Experimental study of β-TCP scaffold loaded with VAN/PLGA microspheres in the treatment of infectious bone defects. *Colloids Surf B Biointerfaces*. 2022;213:112424. doi:10.1016/j.colsurfb.2022.112424
131. Xu W, Tan W, Li C, Wu K, Zeng X, Xiao L. Metformin-loaded β-TCP/CTS/SBA-15 composite scaffolds promote alveolar bone regeneration in a rat model of periodontitis. *J Mater Sci Mater Med*. 2021;32(12):145. doi:10.1007/s10856-021-06621-8
132. Go EJ, Kang EY, Lee SK, et al. An osteoconductive PLGA scaffold with bioactive β-TCP and anti-inflammatory Mg(OH)(2) to improve in vivo bone regeneration. *Biomater Sci*. 2020;8(3):937–948. doi:10.1039/c9bm01864f
133. Cao C, Wang F, Wang EB, Liu Y. [Application of β-TCP for bone defect restore after the mandibular third molars extraction: a split mouth clinical trial]. *Beijing Da Xue Xue Bao*. 2020;52(1):97–102. Dutch. doi:10.19723/j.issn.1671-167X.2020.01.015
134. Han JJ, Chang AR, Ahn J, et al. Efficacy and safety of rhBMP/β-TCP in alveolar ridge preservation: a multicenter, randomized, open-label, comparative, investigator-blinded clinical trial. *Maxillofac Plast Reconstr Surg*. 2021;43(1):42. doi:10.1186/s40902-021-00328-0
135. Wei L, Sun Y, Yu D, et al. The clinical efficacy and safety of ErhBMP-2/BioCaP/β-TCP as a novel bone substitute using the tooth-extraction-socket-healing model: a proof-of-concept randomized controlled trial. *J Clin Periodontol*. 2024:jcpe.14084. doi:10.1111/jcpe.14084
136. Schönegg D, Essig H, Al-Haj Husain A, Weber FE, Valdec S. Patient-specific beta-tricalcium phosphate scaffold for customized alveolar ridge augmentation: a case report: case report: patient-specific β-TCP scaffold for alveolar ridge CBR. *Int J Implant Dent*. 2024;10(1):21. doi:10.1186/s40729-024-00541-2
137. Strauss FJ, Nasirzade J, Kargarpoor Z, Stähli A, Gruber R. Effect of platelet-rich fibrin on cell proliferation, migration, differentiation, inflammation, and osteoclastogenesis: a systematic review of in vitro studies. *Clin Oral Investig*. 2020;24(2):569–584. doi:10.1007/s00784-019-03156-9

138. Baghele O, Thorat M, Malpani P. Clinical and radiographic evaluation of platelet-rich fibrin and bone graft material (β-tricalcium phosphate + hydroxyapatite) in the treatment of intrabony defects of periodontitis patients: a randomized controlled trial. *Quintessence Int*. 2023;54 (6):472–483. doi:10.3290/j.qi.b3920301
139. Tözüm TF, Demiralp B. Platelet-rich plasma: a promising innovation in dentistry. *J Can Dent Assoc*. 2003;69(10):664.
140. Kavitha M, Krishnaveni R, Swathi AM, Abubacker MHM. Evaluation of healing by Cone Beam Computed Tomography (CBCT) using Platelet-Rich Plasma (PRP) + β -Tricalcium Phosphate (β -TCP) and Platelet Rich Fibrin (PRF) + β -Tricalcium Phosphate (β - TCP) in periapical lesions: case report. *Niger J Clin Pract*. 2020;23(7):1026–1029. doi:10.4103/njcp.njcp_54_20
141. Shen G, Ma Y, Zhang S, et al. Osteointegration of PLLA/β-TCP biocomposite anchors used in coracoid transfer procedures for shoulder instability: quantitative computed tomography with a minimum 2-year follow-up. *Orthop J Sports Med*. 2022;10(12):23259671221140901. doi:10.1177/23259671221140901
142. Seebach C, Nau C, Henrich D, et al. Cell-based therapy by autologous bone marrow-derived mononuclear cells for bone augmentation of plate-stabilized proximal humeral fractures: a multicentric, randomized, open phase IIa study. *Stem Cells Transl Med*. 2024;13(1):3–13. doi:10.1093/stcltm/szad067
143. Chu W, Wang X, Gan Y, et al. Screen-enrich-combine circulating system to prepare MSC/β-TCP for bone repair in fractures with depressed tibial plateau. *Regener Med*. 2019;14(6):555–569. doi:10.2217/rme-2018-0047